OREGON GEOLOGY

published by the
Oregon Department of Geology and Mineral Industries

VOLUME 54, NUMBER 2 MARCH 1992

OREGON GEOLOGY

(ISSN 0164-3304)

VOLUME 54, NUMBER 2 MARCH 1992

Published bimonthly in January, March, May, July, September, and November by the Oregon Department of Geology and Mineral Industries. (Volumes 1 through 40 were entitled *The Ore Bin.*)

Main Office: Suite 965, 800 NE Oregon Street # 28, Portland 97232, phone (503) 731-4100, FAX (503) 731-4066.

Baker City Field Office: 1831 First Street, Baker City 97814, phone (503) 523-3133.

Grants Pass Field Office: 5375 Monument Drive, Grants Pass 97526, phone (503) 476-2496. Thomas J. Wiley, Resident Geologist.

Mined Land Reclamation Program: 1534 Queen Ave. SE, Albany 97321, phone (503) 967-2039. Gary W. Lynch, Supervisor.

Second class postage paid at Portland, Oregon. Subscription rates: 1 year, $8; 3 years, $19. Single issues, $2. Available back issues of *Ore Bin/Oregon Geology* through v. 50, no. 4, $1. Address subscription orders, renewals, and changes of address to *Oregon Geology*, Suite 965, 800 NE Oregon Street # 28, Portland 97232.

POSTMASTER: Send address changes to *Oregon Geology*, Suite 965, 800 NE Oregon Street # 28, Portland 97232.

Information for contributors

Oregon Geology is designed to reach a wide spectrum of readers interested in the geology and mineral industry of Oregon. Manuscript contributions are invited on both technical and general-interest subjects relating to Oregon geology. Two copies of the manuscript should be submitted, typed double-spaced throughout (including references) and on one side of the paper only. If manuscript was prepared on common word-processing equipment, an ASCII file copy on 5-in. diskette may be submitted in addition to the paper copies. Graphic illustrations should be camera-ready; photographs should be black-and-white glossies. All figures should be clearly marked, and all figure captions should be typed together on a separate sheet of paper.

The style to be followed is generally that of U.S. Geological Survey publications. (See the USGS manual *Suggestions to Authors*, 7th ed., 1991 or recent issues of *Oregon Geology*.) The bibliography should be limited to references cited. Authors are responsible for the accuracy of the bibliographic references. Names of reviewers should be included in the acknowledgments.

Authors will receive 20 complimentary copies of the issue containing their contribution. Manuscripts, news, notices, and meeting announcements should be sent to Beverly F. Vogt, Publications Manager, at the Portland office of the Oregon Department of Geology and Mineral Industries.

"Lost our lease"—?

Well, no, the Department of Geology and Mineral Industries is still in the State Office Building. But it's the **new** State Office Building, located east of downtown Portland and the Willamette River, just south of the Lloyd Center shopping mall. The map on the cover shows the main approaches and the geographic relation between the old and the new State Office Buildings. See the box above for our new mailing address and phone and FAX numbers. And even before you get to the offices on the 9th floor, you will find, on the ground floor, our new **Nature of Oregon Information Center** (Suite 177), where our maps and other publications will be sold.

MINERAL EXPLORATION ACTIVITY

Regulatory Issues

Final rules implementing the major legislation affecting the permit procedure for heap-leach mining have been adopted by the Department of Geology and Mineral Industries, the Water Resources Department, and the Department of Fish and Wildlife. The Department of Environmental Quality rules for heap-leach-pad liner design, detoxification standards, etc., are undergoing further review prior to being resubmitted to the Environmental Quality Commission for adoption.

Questions or comments should be directed to Gary Lynch or Allen Throop in the Mined Land Reclamation Office of the Oregon Department of Geology and Mineral Industries, 1534 Queen Avenue SE, Albany, OR 97321, telephone (503) 967-2039.

Major mineral exploration activity

No new project applications were received. Because of space limitations in this issue, the table below lists only those projects from the table published in the last (January 1992) issue of *Oregon Geology* that were affected by changes or corrections.

County, date	Project name, company	Project location	Metal	Status
	Permits closed			
Baker 1991	Lower Granview Earth Search Sciences	T. 14 S. R. 37 E.	Gold	App
Harney 1991	Buck Mtn.-North Teck Resources, Inc.	T. 24 S. R. 36 E.	Gold	App
Harney 1991	Adobe Flat Phelps Dodge	T. 28 S. R. 34 E.	Gold	App
Jefferson 1991	Red Jacket Bond Gold	Tps. 9, 10 S. R. 17 E.	Gold	App
Malheur 1990	Calavera NERCO Exploration	T. 21 S. R. 45 E.	Gold	Expl
Malheur 1991	Buck Mtn.-South Teck Resources, Inc.	T. 24 S R. 37 E.	Gold	App
	Changes or corrections in bold print			
Coos 1991	Seven Devils Oreg. Resources Corp.	Tps. 2, 7 S. R. 4 W.	**Chromite, zircon**	Expl com
Malheur 1988	Jessie Page **M.K. Gold Co.**	T. 25 S. R. 43 E.	Gold	Expl
Malheur 1990	Mahogany Project **Cyprus Minerals**	T. 26 S. R. 46 E.	Gold	App
Malheur 1990	Sand Hollow Noranda Exploration	T. 24 S. R. 43 E.	Gold	**Veg**

Explanations: App=application being processed. Expl=Exploration permit issued. Veg=Vegetation permit. Com=Interagency coordinating committee formed, baseline data collection started. Date=Date application was received or permit issued. □

OIL AND GAS NEWS

NWPA schedules symposium and meetings

The Northwest Petroleum Association (NWPA) has scheduled the 1992 annual symposium for October 11-14 in Lincoln City, Oregon. The theme for the symposium is Pacific Northwest Petroleum Development: Geology, geophysics, land, and legal. The symposium chairman is Bob Deacon, consulting geologist. Information can be obtained from the NWPA, P.O. Box 6679, Portland, OR 97228-6679.

The NWPA will hold its next monthly meetings March 13 at the Northwest Natural Gas Building, Portland, and April 10 at the Sweetbriar Inn, Tualatin, Oregon. These meetings are held at 11:30 a.m. and include lunch and a speaker on topics generally relating to energy interests in the Pacific Northwest. Reservations are required and can be made by calling Shelly at (503) 220-2573. □

Geologic guide for the northern Klamath Mountains—Part I Cow Creek to Red Mountain

by M. A. Kays, Department of Geological Sciences, University of Oregon, Eugene, Oregon 97403

This field guide is the first of three parts published for the Geological Society of America (GSA) premeeting field trip no. 1 of the 1992 Cordilleran section meeting. For part 2 (the remainder of Day 1), see the field guide by Donato immediately following this field guide; and for part 3 (Day 2), see Harper (1989). See Figure 1 of this guide for stops of parts 1 and 2.

INTRODUCTION

The northern Klamath Mountains in Oregon consist entirely of accreted terranes (Silberling and others, 1982) that are parts of broader tectonostratigraphic subdivisions referred to as belts (Irwin, 1964). Each arcuately north- to northeast-trending belt is separated from the adjacent by variably east-dipping thrust faults commonly marked by ultramafic rocks. The belts have complex stratigraphic relations, and evidence for upward younging to the northwest is complicated by faulting and folding. According to Hotz (1971a) and Irwin (1985), the terranes of the western Paleozoic-Triassic belt overlie those of the western Jurassic belt approximately along the thrust fault marked by metamorphosed ophiolitic rocks in the area of this field guide (Figures 2 and 3). The thrust fault, referred to here as the Cedar Springs Mountain thrust, continues south more than 250 km into southern Oregon and northern California (Hotz, 1971a). Jachens and others (1986) estimate 110 km of horizontal displacement along the thrust.

The terranes in the area of this field guide have been mapped regionally (Smith and others, 1982) and in more detail (Kays, 1970; Kays and others, 1988). Rock units of the terranes are referred to informally as Cow Creek arc greenstones and mudstones, Elk Creek ophiolitic rocks, and Wildcat Ridge schists and gneisses (see Figure 3). Cow Creek rocks on the west are structurally lowest and are separated from the overlying Elk Creek ultramafic and amphibolitic rocks on the east by the Cedar Springs Mountain thrust fault. Smith and others (1982) correlate the Cow Creek and Elk Creek rocks with the western Jurassic belt and the Wildcat Ridge unit (easternmost) with the western Paleozoic-Triassic belt. On Day 1 of this field trip, we will traverse all the units, paying special attention to their variations in metamorphic grade and degree of structural complexity. As we shall see, these variations relate to the character and timing of metamorphic and deformational events.

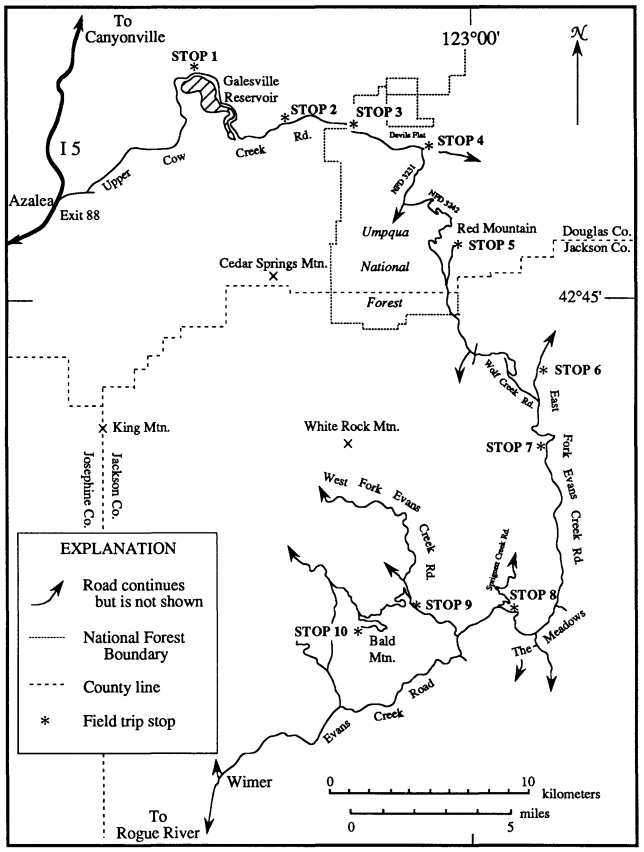

Figure 1. Map showing stops for field trip parts 1 and 2 (Day 1) of premeeting field trip no. 1 of the 1992 Cordilleran section meeting of the Geological Society of America.

TECTONOSTRATIGRAPHIC UNITS

Cow Creek greenstones along the north shore of the Galesville Reservoir near the dam (Stop 1) are flows, breccias, and volcaniclastic andesites-basalts metamorphosed at low grade. Green metatuffs, tuffaceous mudstones, and black, organic-rich mudstones-slates interlayered with the metavolcanic rocks are increasingly abundant 3 to 5 km eastward from the reservoir. Metamorphic grade increases, and fabrics improve in the same direction. Folded black graphitic mudstones-slates (Stop 2) occur on the east beneath the thrust-faulted contact with Elk Creek ophiolitic rocks.

Although offset and locally disturbed by faults, the Cow Creek mudstones, tuffaceous units, and metavolcanic rocks are traceable and locally have recognizable depositional contacts. According to Irwin (1985), the greenstones and mudstones are part of the Western Klamath terrane and the Rogue Valley subterrane (Table 1). In comparison to the descriptions of Wells and Walker (1953) and Garcia (1979, 1982), the Galice Formation fine-grained flysch succession and Rogue Formation metavolcanic rocks are lithologically similar, respectively, to the Cow Creek mudstones and greenstones. Blake and others (1985) indicate that, in the type area, the Galice Formation flysch is depositional on the Rogue Formation tuffs, flows, and volcanic wackes. Thus, the Rogue-Galice relations in the type areas are similar to those of the mudstone-metavolcanic sucession in the Cow Creek sequence (Figure 3). Harper and others (1989) indicate an age range of 150 to 157 Ma for the type Galice Formation, whereas Saleeby (1984) reports an age of 157 ± 2 Ma for dacite dikes in the Rogue Formation. Harper and others (1989) and Pessagno and Blome (1990) indicate that the Galice and Rogue Formations are depositional on the Josephine ophiolite, which is also constrained in age (162 ± 1 Ma, U/Pb zircon age of from plagiogranite).

Elk Creek rocks are penetratively foliated ultramafic schists and amphibolites. The amphibolites (Stop 3) are mafic and locally gradational to coarse-grained clinopyroxene-bearing rocks. Traced southwest, the ultramafic rocks and amphibolites of the Cow Creek

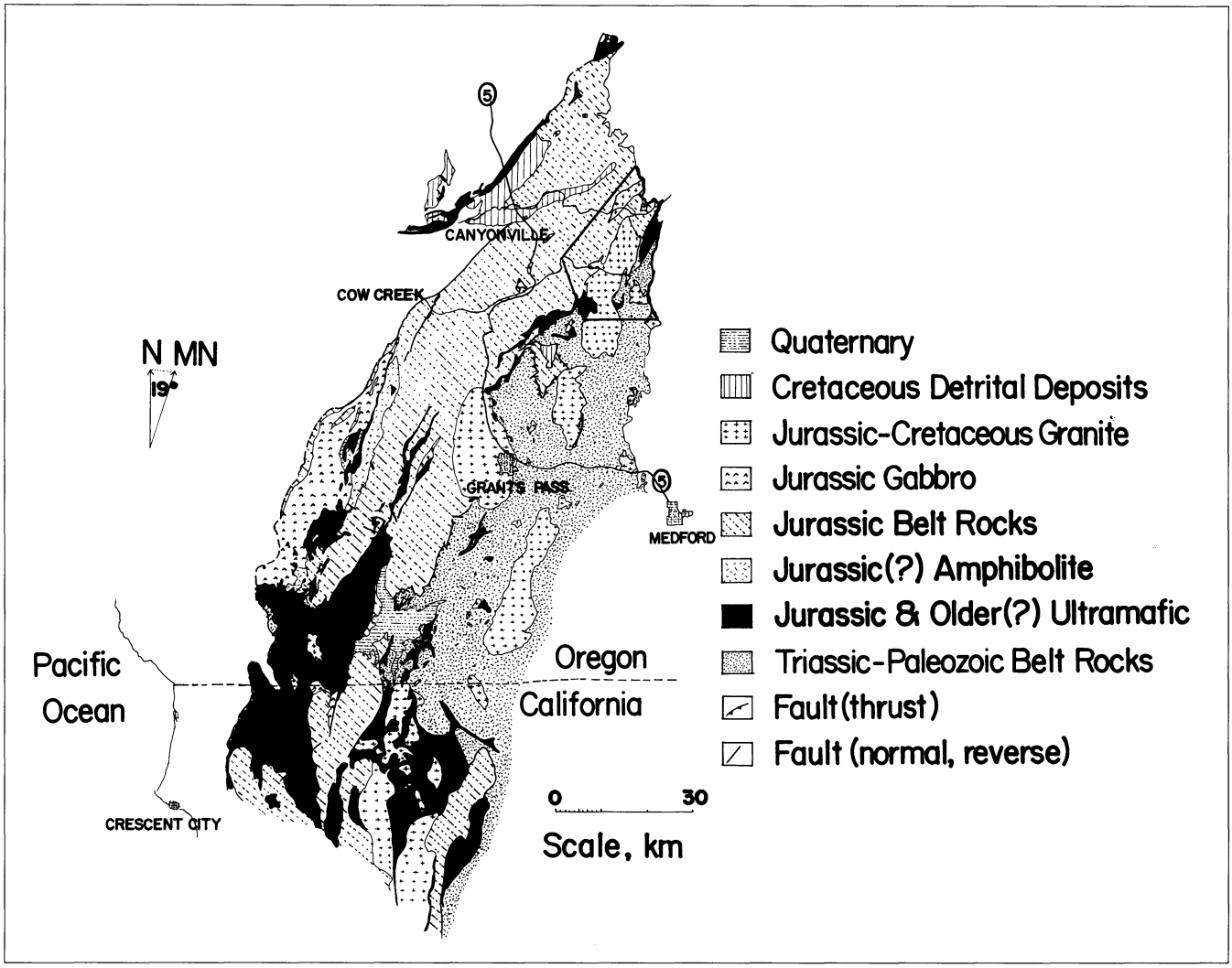

Figure 2. Geologic map, modified from Hotz (1971a), showing geologic units in the western Jurassic and western Paleozoic-Triassic belts in the Klamath Mountains. Circled numbers refer to Interstate 5, which intersects the turnoff eastward on Cow Creek where this field guide begins. The outlined region near the top of the map shows the area under discussion (see text). The northernmost group of Jurassic-Cretaceous plutons (Jurassic-Cretaceous granite) belongs to the White Rock pluton.

area are on line with mapped serpentinized harzburgites, gabbros, diabase dikes, and basalts of the Sexton Mountain area. Smith and others (1982) consider that the ultramafic-mafic suite of Sexton Mountain has "relative" Jurassic age older than the Josephine ophiolite, but no documentation is offered. Irwin (1985) includes Elk Creek rocks with the Rogue Valley subterrane. As we shall see in the following discussion, Elk Creek rock units have textures, structures, and metamorphic characteristics similar to those of the Wildcat Ridge rock units. Elk Creek rocks also occur abundantly as roof pendants and xenolithic rafts within the White Rock pluton. Thus, Elk Creek rocks have questionable terrane affinity, and additional work will be required to properly determine their tectonostratigraphic position.

Wildcat Ridge schists are dominantly mafic, chlorite-actinolite-epidote amphibolites. Locally, there are interlayered quartz-mica and chlorite-quartz schists in addition to narrow belts of tectonically interlayered ultramafic schists. Quartzites and marbles also occur but are rare. The units and their tectonically interlayered nature are similar to those in the Marble Mountains terrane of the western Paleozoic-Triassic belt in the north-central Klamath Mountains (Kays and Ferns, 1980; Mortimore, 1985). The belt extends southward into the Cleveland Ridge quadrangle, where amphibolites are dominant (Smith and others, 1982). All the Wildcat Ridge and Cleveland Ridge rocks have strong metamorphic fabrics. Irwin (1985) correlates these rocks with the May Creek terrane of the Paleozoic-Triassic belt (Table 1). Structurally, the Wildcat Ridge schists are on the downdropped east side of a normal fault that separates these rocks from the underlying Elk Creek ultramafic schists and amphibolites. The normal fault may project into a thrust fault that is largely obscured by intrusion of the White Rock pluton.

White Rock calc-alkaline plutonic rocks intrude Cow Creek, Elk Creek, and Wildcat Ridge rocks. The plutonic rocks are granular, coarse grained, and leucocratic with composition in the range of tonalite-granodiorite-trondhjemite. The more silicic plutonic rocks commonly have white mica and biotite in the mode. Analyzed trondhjemites are peraluminous (2-3 percent normative corundum). The biotite from these rocks gives a corrected K/Ar age of 141 Ma (Hotz, 1971b). The plutonic rocks are only locally foliated (Stop 4), e.g., near contacts with wall rocks and in the vicinity of xenoliths and larger rafts or pendants of the Cow Creek, Elk Creek, and Wildcat Ridge rocks.

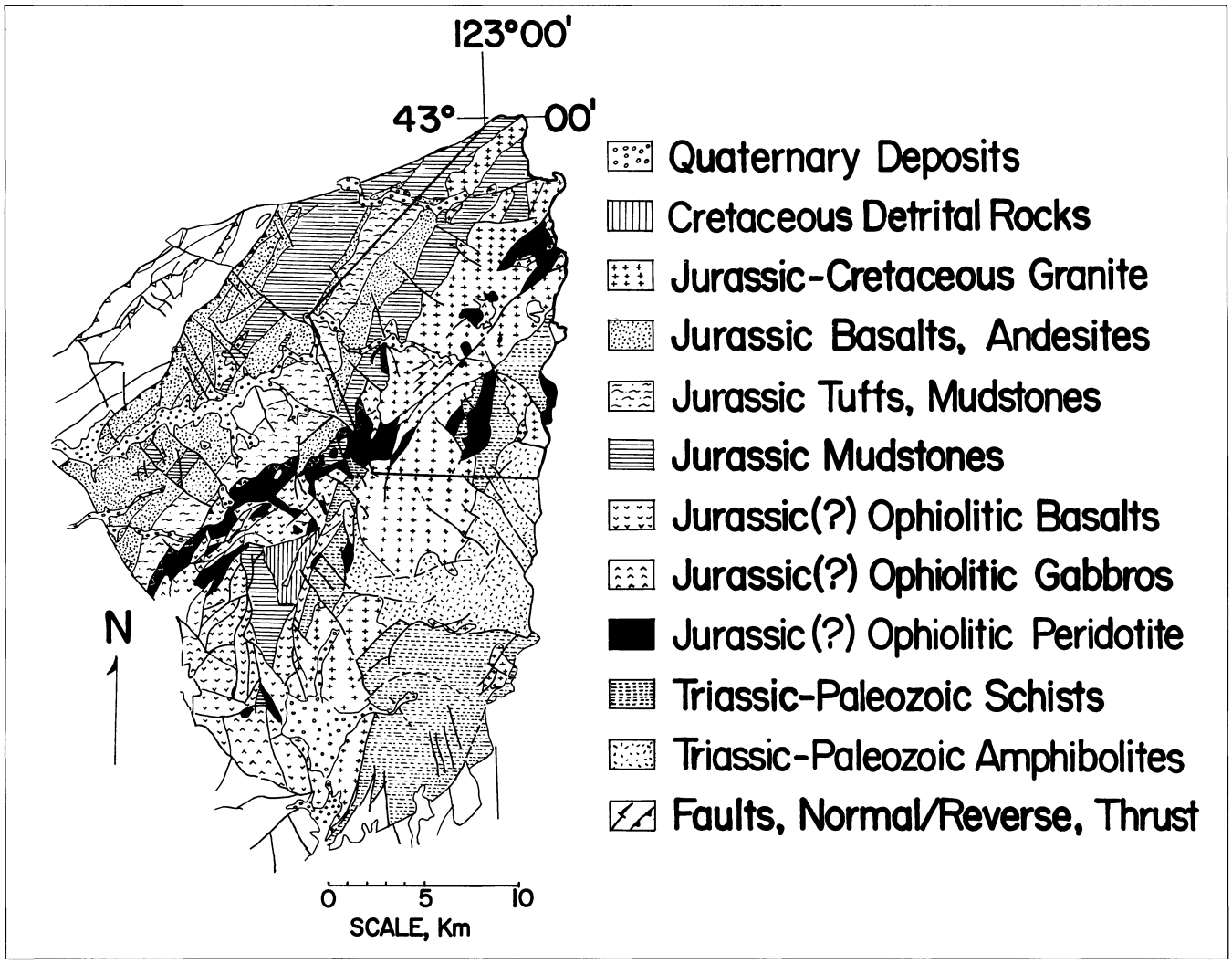

Figure 3. Geologic map for the northern Klamath Mountains, modified in part from Smith and others (1982). The unit "Jurassic-Cretaceous Granite" is referred to in the text as the White Rock pluton. In the area of this field guide (see index boundary), Jurassic basalts, andesites, tuffs, and mudstones are all part of the Cow Creek volcanic-arc mudstone sequence; Jurassic ophiolitic basalts, gabbros, and peridotite are all part of the Elk Creek sequence of rocks; and Triassic-Paleozoic schists and amphibolites are all part of the Wildcat Ridge sequence.

PROGRESSION OF SMALL-SCALE STRUCTURES

D_{1cc}, $D_{1\text{-}2ec}$, and $D_{1\text{-}2wr}$ deformations and related metamorphic structures

The subscripted symbols refer to the conventional ordering of small-scale structures in Cow Creek (cc), Elk Creek (ec), and Wildcat Ridge (wr) rocks. All planar surfaces are referred to by symbol "S," folds by "F," lineations by "L," metamorphic assemblages by "M," and deformations by "D." The metamorphic cleavages/foliations in the three rock groups are all axial planar and are defined relative to the folds that generated them. The earliest recognizable small-scale structure in Cow Creek rocks is well-defined bedding (S_0), which is transposed by penetrative metamorphic cleavage/foliation (S_{1cc}) along the axial planes of outcrop-scale folds (F_{1cc}). The earliest recognizable surface in Wildcat Ridge and Elk Creek rocks is metamorphic layering or cleavage that is transposed in each by a later penetrative metamorphic cleavage/foliation. The subscripts for metamorphic cleavages in Wildcat Ridge and Elk Creek rocks indicate that the earliest foliation assemblage can be distinguished only in the hinge areas of folds, therefore acknowledging that it is not practical to separate these metamorphic surfaces. Therefore, cleavages or foliations in Wildcat Ridge and Elk Creek rocks are termed $S_{1\text{-}2wr}$ and $S_{1\text{-}2ec}$, respectively. These foliations are axial planar to intrafolial folds ($F_{1\text{-}2wr}$ and $F_{1\text{-}2ec}$, respectively) that have millimeter- to centimeter-scale hinges. Overall, the orientations of foliations in Cow Creek (S_{1cc}), Elk Creek ($S_{1\text{-}2ec}$), and Wildcat Ridge ($S_{1\text{-}2wr}$) rocks are parallel. However, because the rock units are separated by faults, cleavages in the separate belts are not necessarily correlative with the same deformation (Table 1).

Quartz-muscovite-chlorite-biotite-feldspars-graphite, and chlorite-actinolite-epidote-plagioclase-oxides ± quartz define the S_{1cc} cleavage in Cow Creek metamudstones-slates and green metatuffs-phyllites, respectively. The cleavage assemblages in Cow Creek black slates and green phyllites record syntectonic M_{1cc} metamorphism. Stop 2 provides an excellent example for observation of metamorphic cleavage (S_{1cc}) that tranposes bedding (S_0) in F_{1cc} fold hinge areas in the black graphitic slates.

Mineral assemblages of Elk Creek foliations ($S_{1\text{-}2ec}$) commonly consist of the following: (1) talc-antigorite-tremolite or talc-olivine-tremolite in ultramafic rocks; (2) actinolitic hornblende-chlorite-plagioclase-epidote/clinozoisite in mafic schists or gneisses, and (3) muscovite-biotite-quartz-graphite-plagioclase ± chlorite in

metamudstones. However, $S_{1\text{-}2ec}$ schistosity in ultramafic rocks of the Elk Creek terrane is difficult to recognize because the rocks are commonly crisscrossed by later anastomosing veins of serpentine. The mineral assemblages of Wildcat Ridge foliations ($S_{1\text{-}2wr}$) are similar to those in micaceous and mafic schists of Elk Creek rocks. Recrystallization syntectonic with deformation $D_{1\text{-}2}$ in Elk Creek and Wildcat Ridge rocks is termed $M_{1\text{-}2ec}$ and $M_{1\text{-}2wr}$, respectively.

D_{2cc}, D_{3ec}, D_{3wr}, and related metamorphic structures

Tonalitic-trondhjemitic plutonic rocks (141 Ma, K/Ar on biotite; Hotz, 1971b) intrude foliated rocks of the Cow Creek, Elk Creek, and Wildcat Ridge groups and are in turn folded by F_{2cc}, F_{3ec}, and F_{3wr} folds, respectively. These deformations also fold intruded, thrust-faulted contacts between Cow Creek and Elk Creek rock groups. Porphyroblastic minerals have a prolonged growth range that is pre- and syntectonic with respect to deformations D_{2cc}, D_{3ec}, and D_{3wr}. Andalusite, staurolite, and locally sillimanite are notable in this regard with elongate crystallographic Z-directions aligned approximately parallel with F_{2cc}, F_{3ec}, and F_{3wr} fold axes. Thus, M_{2cc}, M_{3ec}, and M_{3wr} porphyroblastic assemblages appear to represent one thermal episode that overlapped with D_{2cc}, D_{3ec}, and D_{3wr} deformations, respectively, in the three rock groups. Consequently, alignment of porphyroblasts in pelitic schists and finer grained amphibole in amphibolites forms a lineation (L_{2cc}, L_{3ec}, L_{3wr}) in Cow Creek, Elk Creek, and Wildcat Ridge rocks, respectively. A penetrative cleavage/foliation did not form during this recrystallization.

Later structures

All rock units have been broadly folded (F_{3cc}, F_{4ec}, and F_{4wr}, etc., in the Cow Creek, Elk Creek, and Wildcat Ridge terranes, respectively) and were subsequently faulted. These tectonic events are generally unconstrained in age, except where metamorphic rocks are overlain by Upper Cretaceous sedimentary rocks and/or Eocene volcanic rocks of the western Cascades. For example, faults later than latest folding are pre- and post-Western Cascade (Eocene-Oligocene?) deposition.

METAMORPHISM

Structural observations on small-scale structures indicate that metamorphic assemblages in all three terranes are polymetamorphic. The porphyroblastic (M_{2cc}, M_{3ec}, and M_{3wr}) assemblages are independent of boundaries between the Cow Creek, Elk Creek, and Wildcat Ridge rock units (Kays and Rice, 1991).

The mapped facies boundaries shown in Figure 4 are based on mineral assemblages in metapelitic rocks. More detailed subdivision is possible and includes: (1) chlorite, (2) chlorite-biotite, (3) andalusite-biotite-chlorite, (4) andalusite-staurolite-chlorite, and (5) staurolite-sillimanite zones. Zone 1 is broadest and is mostly outside the area of detailed mapping in Figure 4. Within it, assemblages vary from incompletely recrystallized with nonpenetrative fabrics to completely recrystallized slates and phyllites. Assemblages in zones 2-5 are phyllitic to schistose and are illustrated by the use of AFM diagrams (Figure 5). The staurolite-sillimanite zone assemblages are widespread in the area of abundant plutonic rocks and may represent assemblages formed in (now eroded) roof pendants. The structural data seem to confirm this idea. Overall, metamorphic assemblages in the serpentinized ultramafic rocks and in mafic amphibolite gneisses are consistent with those in the metapelites.

INTERPRETATION OF METAMORPHIC ASSEMBLAGES AND SMALL-SCALE STRUCTURES

Metamorphic assemblages form cleavages/foliations S_{1cc}, $S_{1\text{-}2ec}$, and $S_{1\text{-}2wr}$, respectively, in the Cow Creek, Elk Creek, and Wildcat Ridge rock units. These foliations are earlier than the White Rock pluton with a cooling age of 141 Ma (K/Ar on biotite; Hotz, 1971b).

Table 1. *Subdivision of the terranes of the northern Klamath Mountains*

Postamalgamation pluton	Belt	Terrane	Subterrane	Lithotectonic units	Small-scale structures
Jurassic-Cretaceous White Rock pluton (141 Ma, K/Ar on biotite)				Tonalite-trondhjemite-granodiorite with two micas, peraluminous	Locally foliated in xenoliths or roof pendants, syntectonic with F_{2cc}; F_{3ec}, F_{3wr}.
	Western Jurassic belt				
		Western Klamath terrane			
			Rogue Valley subterrane	Cow Creek greenstones-amphibolites, mudstones-slates-schists	S_0; S_{1cc}, F_{1cc}, L_{1cc}; F_{2cc}, L_{2cc}.
	(?)	(?)	(?)	Elk Creek ultramafic schists, amphibolites (terrane affinity still in question)	$S_{1\text{-}2ec}$, $F_{1\text{-}2ec}$, $L_{1\text{-}2ec}$; F_{3ec}, L_{3ec}.
	Paleozoic-Triassic belt				
		May Creek terrane		Wildcat Ridge schists (melange?), amphibolite, chlorite-quartz, quartz-biotite, serpentine-talc-tremolite schists	$S_{1\text{-}2wr}$, $F_{1\text{-}2wr}$, $L_{1\text{-}2wr}$; F_{3wr}, L_{3wr}.

Notes:
—S_{1cc}, $S_{1\text{-}2ec}$ are subparallel to the Cedar Springs Mountain thrust fault separating terranes and lithotectonic units; $S_{1\text{-}2ec}$, $S_{1\text{-}2wr}$ foliations are largely parallel.
—The White Rock pluton intrudes S_{1cc}, $S_{1\text{-}2ec}$, $S_{1\text{-}2wr}$.
—Final recrystallization and porphyroblastic mineral growth was syntectonic with F_{2cc}, F_{3ec}, F_{3wr}, and these assemblages are prograde toward the White Rock pluton.

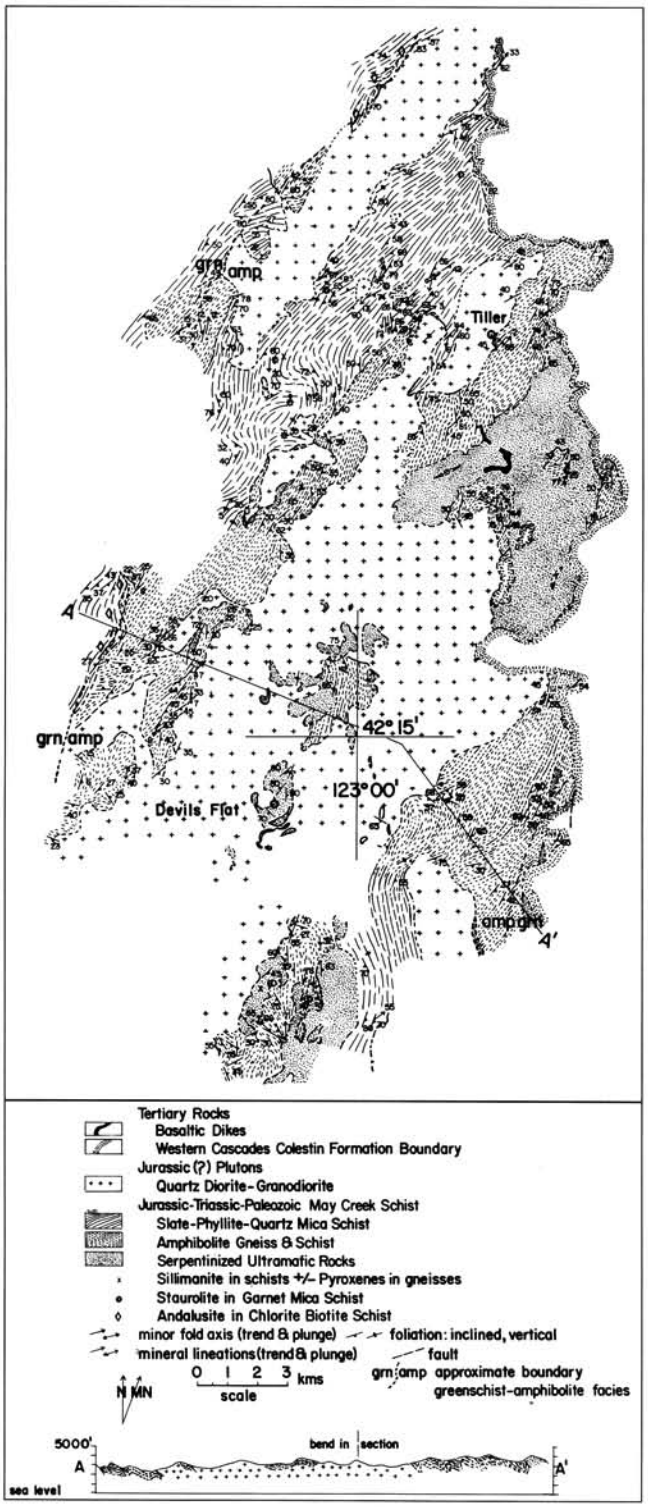

Figure 4. Geologic map for the northern Klamath Mountains, modified from Kays (1970); Kays and others (1988); and later work by Kays. The metamorphic zone boundary indicated as "grn:amp" is approximately the greenschist-amphibolite facies boundary separating assemblages in the andalusite-biotite-chlorite zone from those in the andalusite-staurolite-chlorite zone or the sillimanite-staurolite-biotite zone in metapelitic slates and schists. See Figures 2 and 3 for terrane affinities of the metamorphic map units that are shown here.

However, the cooling age is nearly the same as the magmatic age of the Grants Pass pluton (139 Ma, U/Pb on zircon; Harper and others, 1989), which has a composition and structural positioning that is similar to the White Rock pluton. Correlation of Cow Creek rocks with those of the Galice and Rogue Formations (Smith and others, 1982) with an age range of 150-162 Ma (Harper and others, 1989) makes S_{1cc} foliation younger than this range but older than 141 Ma. Penetrative foliations in the Elk Creek ($S_{1\text{-}2cc}$) and Wildcat Ridge ($S_{1\text{-}2wr}$) metamorphic rocks are also older than 141 Ma but transpose an even older metamorphic fabric. These relations indicate that if Cow Creek metamorphism (M_{1cc}) is Nevadan (older than 141 Ma and younger than 150-160 Ma), then the earliest unconstrained Elk Creek and Wildcat Ridge metamorphic fabrics could be pre-Nevadan (Siskiyou event of Coleman and others, 1988). Penetrative Elk Creek and Wildcat Ridge foliations are also unconstrained with regard to their maximum age. However, Donato and Lanphere (1992) have recently obtained a U/Pb zircon age of approximately 154 Ma on diorite that intrudes an amphibolite unit structurally below the May Creek Schist in the western Paleozoic-Triassic belt south of Wildcat Ridge. The suggestion is that metamorphic foliation in the Wildcat Ridge rocks, which Irwin (1985) assigns to May Creek terrane (western Paleozoic-Triassic belt), could be "earliest" Nevadan or pre-Nevadan.

Field and petrographic data suggest that the final prograde metamorphic event included a porphyroblastic growth stage that was achieved by overprinting the minerals that formed penetrative cleavage/foliation. Furthermore, this porphyroblastic recrystallization (termed M_{2cc}, M_{3ec}, and M_{3wr} in Cow Creek, Elk Creek, and Wildcat Ridge rocks, respectively) overlapped with isoclinal (F_{2cc}, F_{3ec}, and F_{3wr}) folding. Equivalence of these metamorphisms indicates a metamorphic field gradient for the last metamorphic event that proceeded along a prograde, low-pressure path largely in the andalusite stability field. The path crossed into the sillimanite field at pressures less than the triple point for the Al_2SiO_5 polymorphs (about 3.8 kbars). The narrow width of mapped metamorphic zones in the andalusite field suggests a rapidly rising temperature that culminated in a broader amphibolite facies (staurolite-sillimanite zone) in more abundantly intruded rocks (Figure 4).

As noted in the discussion of small-scale structures, porphyroblastic growth that overlapped with F_{2cc}, F_{3ec}, and F_{3wr} folding was synchronous with or followed intrusion of tonalite-trondhjemite plutons in the region. The chronology of structures and assemblages and their distribution argues in favor of a regional, prograde sequence that formed later than the Cedar Springs Mountain thrust. Furthermore, assemblages in metapelites and their progression are not the same as the kyanite-sillimanite or andalusite-sillimanite baric types. The suggestion is that the assemblages are representative of an intermediate metamorphic path that is typical of metamorphism in the northern Klamath Mountains of Oregon. The cooling age (141 Ma, K/Ar on biotite; Hotz 1971b) for the White Rock pluton indicates that this metamorphism is Nevadan.

REFERENCES CITED

Blake, M.C., Jr., Engebretson, D.C., Jayko, A.S., and Jones, D.L., 1985, Tectonostratigraphic terranes in southwest Oregon, *in* Howell, D.G., ed., Tectonostratigraphic terranes of the circum-Pacific region: Circum-Pacific Council for Energy and Mineral Resources: Earth Science Series, v. 1, p. 147-157.

Coleman, R.G., Manning, C.E., Donato, M.M., Mortimer, N., and Hill, L.B., 1988, Tectonic and regional metamorphic framework of the Klamath Mountains and adjacent Coast Ranges, California and Oregon, *in* Ernst, W.G., ed., Metamorphism and crustal evolution of the western United States, Rubey Volume 7 (Papers presented at the Rubey Colloquium, University of California, Los Angeles, January 1986): Englewood Cliffs, N.J., Prentice-Hall, p. 1061-1097.

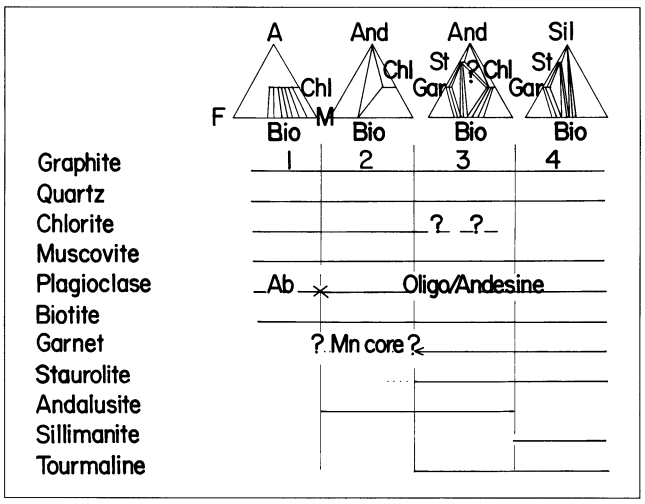

Figure 5. Metamorphic assemblages in metapelitic slates and schists in the northern Klamath Mountains. Zones 1 and 2 are greenschist facies; zones 3 and 4 are amphibolite facies.

Donato, M.M., and Lanphere, M.M., 1992, Geochronologic studies of selected amphibolites in the northern Klamath Mountains: Geological Society of America Abstracts with Programs, v. 24.

Garcia, M.O., 1979, Petrology of the Rogue and Galice Formations, Klamath Mountains, Oregon: Identification of a Jurassic island arc: Journal of Geology, v. 87, no. 1, p. 29-41.

———1982, Petrology of the Rogue River island-arc volcanic complex, southwest Oregon: American Journal of Science, v. 282, p. 783-807.

Harper, G.D., 1989, Geologic evolution of the northernmost Coast Ranges and western Klamath Mountains, California: American Geophysical Union Field Trip Guidebook T308, p. 1-20.

Harper, G.D., Saleeby, J.B., Pessagno, E.A., Jr., and Heizler, M., 1989, The Josephine ophiolite: generation, translation, and emplacement of a Late Jurassic parautochthonous back-arc lithosphere, Klamath Mountains, California-Oregon [abs.]: Geological Society of America Abstracts with Programs, v. 21, no. 6, p. A28.

Hotz, P.E., 1971a, Geology of lode gold districts in the Klamath Mountains, California and Oregon: U.S. Geological Survey Bulletin 1290, 91 p.

———1971b, Plutonic rocks of the Klamath Mountains, California and Oregon: U.S. Geological Survey Professional Paper 684-B, 20 p.

Irwin, W.P., 1964, Late Mesozoic orogenies in the ultramafic belts of northwestern California and southwestern Oregon: U.S. Geological Survey Professional Paper 501-C, p. C1-C9.

———1985, Age and tectonics of plutonic belts in accreted terranes of the Klamath Mountains, California and Oregon, *in* Howell, D.G., ed., Tectonostratigraphic terranes of the circum-Pacific region: Circum-Pacific Council for Energy and Mineral Resources: Earth Science Series, v. 1, p. 187-199.

Jachens, R.C., Barnes, C.G., and Donato, M.M., 1986, Subsurface configuration of the Orleans fault: Implications for deformation in the western Klamath Mountains, California: Geological Society of America Bulletin, v. 97, no. 4, p. 388-395.

Kays, M.A., 1970, Mesozoic metamorphism, May Creek Schist belt, Klamath Mountains, Oregon: Geological Society of America Bulletin, v. 81, no. 9, p. 2743-2758.

Kays, M.A., and Ferns, M.L., 1980, Geologic field trip guide through the north-central Klamath Mountains: Oregon Geology, v. 42, no. 2, p. 23-35.

Kays, M.A., Ferns, M.L., and Brooks, H.C., 1988, Metamorphism of Triassic-Paleozoic belt rocks: a guide to field and petrologic relations in the oceanic melange, Klamath and Blue Mountains, California and Oregon, *in* Ernst, W.G., ed., Metamorphism and crustal evolution of the western United States, Rubey Volume 7 (Papers presented at the Rubey Colloquium, University of California, Los Angeles, January 1986): Englewood Cliffs, N.J., Prentice-Hall, p. 1098-1142.

Kays, M.A., and Rice, J.M., 1991, Prograde Nevadan metamorphism in the northern Klamath Mountains, Oregon [abs.]: Geological Society of America Abstracts with Programs, v. 23, no. 5, p. 248.

Mortimore, N., 1985, Structural and metamorphic aspects of Middle Jurassic terrane juxtaposition, northeastern Klamath Mountains, California, *in* Howell, D.G., ed., Tectonostratigraphic terranes of the circum-Pacific region: Circum-Pacific Council for Energy and Mineral Resources: Earth Science Series, v. 1, p. 201-214.

Pessagno, E.A., Jr., and Blome, C.D., 1990, Implications of new Jurassic stratigraphic, geochronometric, and paleolatitudinal data from the western Klamath terrane (Smith River and Rogue Valley subterranes): Geology, v. 18, no. 7, p. 665-668.

Ramp, L., 1972, Geology and mineral resources of Douglas County, Oregon: Oregon Department of Geology and Mineral Industries Bulletin 75, 106 p.

Saleeby, J.B., 1984, Pb/U zircon ages from the Rogue River area, western Jurassic belt, Klamath Mountains, Oregon [abs.]: Geological Society of America Abstracts with Programs, v. 16, no. 5, p. 331.

Silberling, N.J., Jones, D.L., Blake, M.C., Jr., and Howell, D.G., 1987, Lithotectonic terrane map of the western conterminous United States: U.S. Geological Survey Miscellaneous Field Studies Map MF-1874-C, 20 p., map scale 1:2,500,000.

Smith, J.G., Page, N.J., Johnson, M.G., Moring, B.C., and Gray, F., 1982, Preliminary geologic map of the Medford 1° by 2° quadrangle, Oregon and California: U.S. Geological Survey Open File Report 82-955, scale 1:250,000.

Wells, F.G., and Walker, G.W., 1953, Geologic map of the Galice quadrangle, Oregon: U.S. Geological Survey Geological Quadrangle Map GQ-25, scale 1:62,500.

FIELD LOG—DAY 1, PART 1, COW CREEK TO RED MOUNTAIN

For the GSA field trip, a handout log without details is provided for the transit along Interstate 5 to the start of the guided field trip. General geology for the log on Interstate 5 is from Ramp (1972). For stops on Day 1, see Figure 1.

Milepoint 0.0—Start. Field log for Day 1 begins at intersection of Interstate 5 with Cow Creek Road (107.2 mi from Eugene) after taking Azalea Exit 88 going east to Galesville Reservoir.

7.2—Stop 1. Galesville Reservoir pullout on right. The Cow Creek terrane low-grade green metatuffs and volcaniclastic breccias are considered equivalent in age to the Upper Jurassic Rogue and Galice Formations (Smith and others, 1982). Deformation is by brittle cataclasis but may be ductile-brittle in the metatuffs. Tensional veins in the volcaniclastic rocks are filled with clinozoisite fibers. The fibers are aligned parallel to shear planes with orientation N. 6° E., 53° SE. Fiber alignment and shear planes are at high angle to tensional veins. Shear sense is top to west.

12.6—Stop 2. Well-exposed outcrop-scale folds (F_{1cc}) of Cow Creek mudstone-slate with penetrative axial planar cleavage (S_{1cc}). The cleavage assemblage is muscovite-quartz-chlorite-graphite ± albite and transposes bedding (rhythmic organic mudstone-quartzose siltstone layers). The F_{1cc} fold axes are N. 3° E. to N. 35° E., plunging 11° to 18°. The folds are faulted. The S_{1cc} cleavage is folded by smaller scale folds (F_{2cc}). Folds of bedding (S_0) distinguish Cow Creek mudstones from Elk Creek and Wildcat Ridge rocks.

15.1—Stop 3. Elk Creek terrane amphibolite gneiss outcrop and borrow pit for road rock. The rock is composed of medium-grained amphibole, plagioclase (An_{22}), and lesser amounts of sphene and/or rutile and clinozoisite-epidote. Note that there are abundant small-scale, sheared, intrafolial ("fish-hook" $F_{1\text{-}2ec}$) folds. The wavelengths of the sheared $F_{1\text{-}2ec}$ folds are several millimeters to a centimeter in the hinge areas. The folds trend N. 25° E. to N. 35° E. and plunge 0° to 35°. Penetrative $S_{1\text{-}2ec}$

foliation is axial planar to the intrafolial folds and transposes earlier, poorly defined cleavage or foliation and feldspar-quartz segregation veins. The veins when folded form ptygma that also define $F_{1\text{-}2ec}$ hinges. Locally, there are larger scale F_{3ec} isoclinal folds of foliation. Note the contrast between the style of $F_{1\text{-}2ec}$ and F_{1cc} folds (Stop 2).

17.6—STOP 4. Coarse-grained, two-mica granodiorite with well-developed foliation (approximately N. 10° E., 40° SE.) that consists of mica, quartz, and feldspar alignment and a slight segregation of biotite. Larger feldspar grains are augen shaped, and there are crushed quartz and feldspar grains indicating shearing. See especially the large xenoliths of serpentinized peridotite and amphibolite gneiss and the foliation in the gneiss (N. 25° E., 35° SE.) subparallel to that of granodiorite. See also the broken fold in the amphibolite with an upper sheared limb to the west.

18.0—Devils Flat picnic area (turn left over cattle guard). Lunch stop for GSA field trip. Those who are interested may continue 0.2 mi east on Upper Cow Creek Road for a closer look at the granodiorite and its locally abundant xenoliths. At this location we are well inside the pluton and the foliation here, in contrast to that recognized in the granodiorite at Stop 4, is poor except immediately adjacent to the larger xenoliths of amphibolite and serpentinized peridotite. The trend of the foliation in the xenoliths is generally concordant with that of metamorphic rocks adjacent to the pluton, although it is clear that plutonic rocks intrude the metamorphic foliation.

After lunch stop at Devils Flat, turn around and drive back about 0.4 mi to Stop 4 and then turn left (south) onto Applegate Creek Road.

17.6—Continue south on Applegate Creek Road or NFD (National Forest Road) 3231, traveling through weathered granodiorite with large and small rafts of serpentinized peridotite, amphibolite, and occasional biotite-rich schist.

19.7—Turn left at road intersection with NFD 3242 to Red Mountain and stay on 3242. The road cuts are mainly granodiorite with xenoliths of ultramafic rocks, schist, and amphibolite of the Elk Creek terrane for the first approximately 1.2 mi, until we reach the contact between metamorphic and plutonic rocks.

26.3—Continue along NFD 3242 in ultramafic rocks and occasional amphibolite to the next road intersection.

27.8—Turn left at road intersection NFD 3242 and spur road 230 to Red Mountain. The rocks at the intersection are sheared talc-tremolite serpentinites with a spaced cleavage parallel to shear planes.

28.0—Road metal quarry in massive serpentinite. Just ahead there are mafic metasomatized (rodingitic?) amphibole-rich "dikes" in the serpentinite.

29.2—Stop 5. Former site of Red Mountain Lookout, where serpentinized peridotite and amphibolite are in contact. The contact trends approximately NS to NW and may be a recrystallized and subsequently folded thrust. The peridotite consists of (approximately 10- x 40-cm) phacoidal blocks that are bounded by anastomosing veins of sheared talc-tremolite serpentinite. Internally, the peridotite has penetrative cleavage caused by preferred orientation or alignment of antigorite and talc and lesser amounts of chlorite and tremolite. The cleavage is interpreted to be $S_{1\text{-}2ec}$ but is easily modified or disturbed and in some places obliterated by the anastomosing veins. In some places the veins are planar shear zones centimeters to several centimeters thick and form a spaced cleavage (N. 57° E., 72° SE.) that transposes $S_{1\text{-}2ec}$ in the peridotite. The amphibolite is amphibole rich with 1 mm thick or less lensoidal plagioclase- and amphibole-rich bands. The banding and flattened amphibole grains constitute $S_{1\text{-}2ec}$.

Return 1.2 mi to intersection of NFD 230 and NFD 3242 for part 2 of the field trip (discussion by Donato, next page).

Field trip continues on next page →

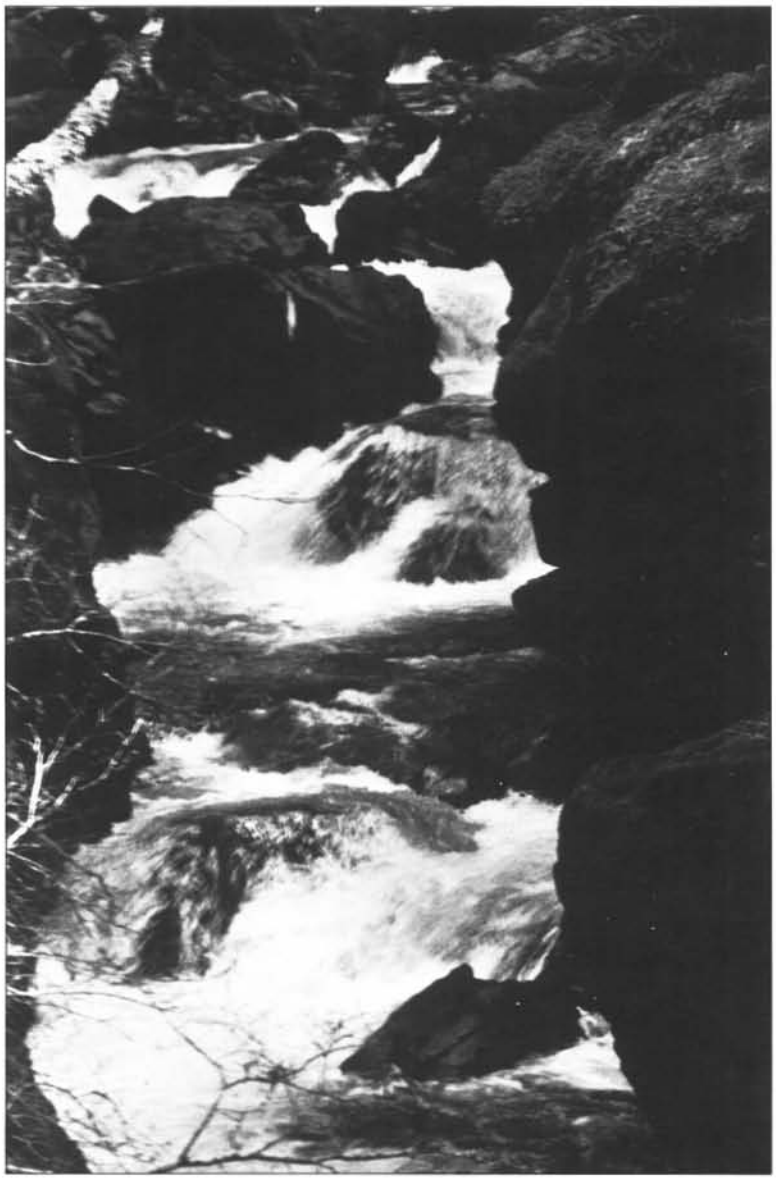

Cow Creek Gorge at Devils Flat. This is the area of the lunch stop for the Klamath Mountains field trip that is premeeting field trip 1 of the 1992 Cordilleran Section meeting of the Geological Society of America. Photo courtesy of Jim Hines, Tiller Ranger Station, Umpqua National Forest, USDA Forest Service.

Geologic guide for the northern Klamath Mountains—Part 2
Red Mountain to Bald Mountain (May Creek Schist and related rocks)

by Mary M. Donato, U.S. Geological Survey, MS 910, 345 Middlefield Road, Menlo Park, California 94025

INTRODUCTION

The second part of this field trip highlights selected localities in amphibolite-facies metabasites (amphibolites) and structurally overlying metasedimentary rocks known as the May Creek Schist (usage of Donato, 1991b). The route generally traverses the area from north to south and from lower to higher structural levels, beginning in amphibolite and ending in mylonitic May Creek Schist.

The amphibolite and the May Creek Schist crop out in the northeasternmost part of the Klamath Mountains and are part of Irwin's (1966) western Paleozoic and Triassic belt, although this name probably does not accurately describe the age of these rocks (see below). Their location and distribution are shown in Figure 1. These units are noteworthy because they are distinctly higher grade than the predominantly greenschist-facies rocks in this part of southwestern Oregon. Most contacts with adjacent units are faults, or they are obscured by intrusive bodies.

Neither the protolith age nor the metamorphic age of these rocks is well known, but a few constraints are available. The White Rock pluton (141 Ma; K/Ar, biotite; Hotz, 1971) clearly intrudes and contact-metamorphoses the amphibolite. The Wimer pluton, which intrudes both the May Creek Schist and the amphibolite, is undated but may be similar in age to the nearby Grants Pass pluton (139 Ma; Saleeby, 1984).

Initial $^{40}Ar/^{39}Ar$ incremental heating studies on metamorphic hornblendes from the amphibolite suggested a so-called Nevadan cooling age of approximately 145 Ma (Donato, 1991a), but continuing work has yielded plateau ages ranging from approximately 111 Ma to approximately 162 Ma (Donato, unpublished data). A syntectonic hornblende diorite that concordantly intrudes, contact-metamorphoses, and engulfs xenoliths of amphibolite near the contact with the May Creek Schist gives igneous (Pb/U, zircon; Richard Tosdal, U.S. Geological Survey, written communication, 1991) and cooling ($^{40}Ar/^{39}Ar$, hornblende; Donato, unpublished data) ages of approximately 154 Ma and 153 Ma, respectively. Contact relations and textures suggest that emplacement of the diorite postdated or was synchronous with the later stages of metamorphism and deformation of the amphibolite. The diorite exhibits "hot-worked" narrow shear bands composed of polygonized hornblende and plagioclase, which indicates that it continued to be deformed at high temperature after its emplacement (see Stop 9, below). Clearly, the amphibolite and related intrusive rocks have complicated thermal and deformational histories, and resolving them will require further work.

AMPHIBOLITE

The unnamed amphibolite that structurally underlies the May Creek Schist (Figure 2) consists primarily of dark-greenish-gray to black, well-foliated and lineated hornblende-plagioclase schist and gneiss. Although the amphibolite is typically strongly deformed, relict igneous textures are preserved locally in less deformed rocks. Note, however, that all rocks discussed here are thoroughly metamorphosed and recrystallized.

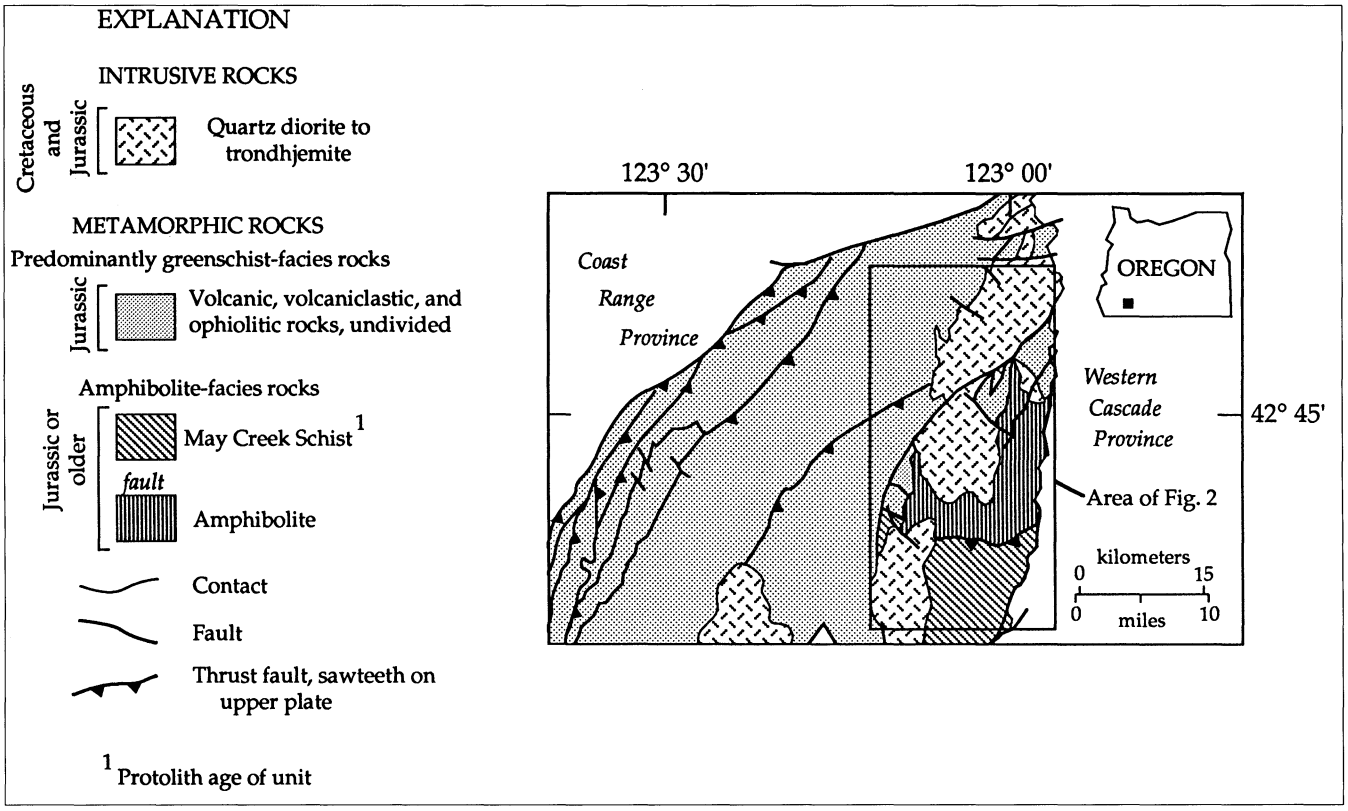

Figure 1. Generalized geologic map of the northeastern Klamath Mountains. Geology after Smith and others (1982).

In addition to the abundant "common" amphibolite (amphibole schist), several textural varieties of amphibolite, including metaporphyry, metadiorite, and metagabbro (so named for their apparent igneous protoliths) have been recognized. In places, tabular bodies of different textural varieties (e.g., metaporphyry vs. metadiorite) are separated by sharp planar contacts, which suggests that they are metamorphosed sheeted dikes or sills (examples at Stops 6 and 7).

All varieties of amphibolite have essentially the same mineralogy: magnesio-hornblende + intermediate plagioclase + accessory sphene ± Fe-Ti oxide. Chlorite and epidote are rarely observed; garnet is absent. Middle-amphibolite-facies metamorphic temperatures and low to moderate pressures are indicated. More complete descriptions of the various types of amphibolite are given in Donato (1991a; 1991b).

The amphibolite contains structurally concordant, massive to schistose bodies of metamorphosed ultramafic rocks (metaserpentinite) that range in size from less than 1 m to 2-3 km in largest dimension. Mineral assemblages include olivine + antigorite + chlorite + opaque oxide (probably magnetite) and olivine + tremolite + chlorite, thus indicating that the ultramafic rocks are the same metamorphic grade as the enclosing amphibolite. Indeed, blackwall (chlorite-talc-magnetite) rinds around metaserpentinite suggest that metamorphism of amphibolite and serpentinite was synchronous. No metamorphosed rodingites were found, however, which suggests that the ultramafites were tectonically incorporated as serpentinites and were not serpentinized *in situ*.

The geochemical characteristics, particularly trace-element compositions, of the amphibolite are very similar to those of present-day oceanic basalts, particularly basalts erupted in back-arc basins (Donato, 1991b). The oceanic geochemical signature of the amphibolite and its present structural position east of Jurassic arc volcanic and volcaniclastic rocks together suggest that the amphibolites formed in a back-arc basin environment.

The amphibolites are L-S tectonites with a pervasive schistosity or foliation defined by alternating hornblende- and plagioclase-rich layers. The foliation generally dips southeast, although it is broadly warped on regional and local scales. A strong, consistent, southeast-plunging hornblende lineation is also present throughout. In some cases, elongate, recrystallized plagioclase grains or aggregates define a measurable flattening plane or, rarely, a stretching lineation parallel to the hornblende lineation. Foliation and lineation in the amphibolite become more pronounced near the contact with the overlying May Creek Schist, but shear criteria and textural evidence of intense ductile deformation and dynamic recrystallization are best developed in the basal, quartzose part of the May Creek Schist.

Rare outcrop-scale isoclinal reclined folds deform the foliation. These folds generally plunge southeast, parallel to the hornblende lineation and parallel to stretching lineations measured in metasedimentary rocks from the ductile shear zone; the axial planes of reclined folds are parallel to the measured foliation.

MAY CREEK SCHIST

Mica schist and mica slate considered to be Devonian(?) in age and located near the town of Wimer, Oregon, were named the May Creek Formation by Diller and Kay (1924). Today the name "May Creek Schist" refers to rocks corresponding in part to Diller and Kay's (1924) May Creek Formation (see Donato, 1991b). The May Creek Schist structurally overlies the amphibolite along a ductile shear zone, described below. The nature of the original contact is unknown, but the protolith of the May Creek Schist may have been deposited directly on the basaltic protolith of the amphibolite.

The May Creek Schist shows considerable compositional variety. The lower structural levels are generally quartz rich and include nearly pure quartzite, quartz-biotite schist, and quartzofeldspathic schist, consisting mainly of quartz, feldspar, biotite, and white mica with accessory garnet, tourmaline, opaque oxides, and amphibole. Calcareous schists containing quartz, clinozoisite, sphene, and calcite are also present. At higher structural levels (mostly south of Evans Creek; not covered by this road log), schists are less siliceous, are more amphibole- and biotite-rich, and contain apparent volcanic detritus as well as more abundant calcareous material. Petrographic examination of these rocks shows abundant plagioclase along with biotite, quartz, amphibole, diopside, and accessory amounts of distinctive rose-colored sphene. Potassium feldspar (microcline) is abundant in some samples.

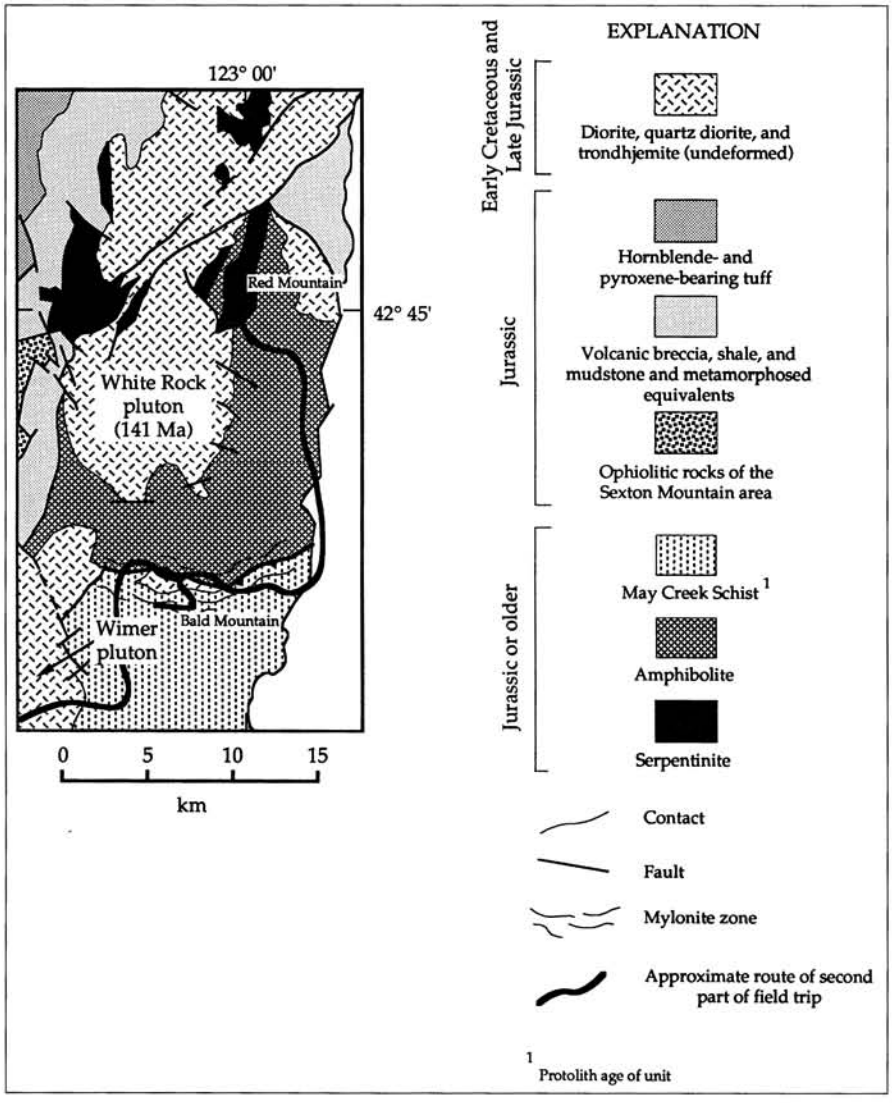

Figure 2. Simplified geologic map showing part of the May Creek Schist and underlying amphibolite in the area covered by the road log. Heavy black line shows approximate route taken by this part of the field trip. Refer to map in companion paper by Kays (above, page 27) for complete route. Geology after Smith and others (1982) and Donato (1991b).

Diagnostic metamorphic mineral assemblages are rare in the metasedimentary rocks in this area. Sillimanite occurs with quartz, plagioclase, biotite, garnet, and white mica at two known localities. Lensoidal aggregates of white mica in samples close to plutonic bodies may represent former contact-metamorphic andalusite or staurolite porphyroblasts. No regional metamorphic andalusite or staurolite was observed in this area, but this lack may only reflect bulk rock composition. In the more calcic tuffaceous rocks higher in the section, diopside coexists with plagioclase, quartz, amphibole, biotite, and calcite. Attempts to establish metamorphic temperatures in four samples of pelitic rocks by using garnet-biotite geothermometry yielded inconsistent results ranging from near 550 °C to nearly 900 °C, with most determinations in the 550° to 650° range (Donato, 1991b). Therefore, although it is impossible to closely constrain temperature and pressure with the available assemblages, middle amphibolite-facies conditions are generally indicated.

The May Creek Schist is everywhere well foliated but is strongly lineated only near its base where it has undergone intense ductile deformation. In pelitic, semipelitic, and psammitic varieties, foliation is defined by alternating micaceous and quartzofeldspathic layers and by flattened lensoidal aggregates of plagioclase or mica. Rocks within the ductile shear zone display a conspicuous lineation caused by elongated quartz, feldspar, and mica grains within the foliation plane. Structural elements such as foliation and lineation in the May Creek Schist are generally parallel to those in the amphibolite (Donato, 1990 and in preparation).

DUCTILE SHEAR ZONE

A zone of ductilely deformed quartz-mica schist and quartzofeldspathic gneiss marks the basal part of the May Creek Schist and indicates northwestward transport of the May Creek Schist over the amphibolite (Donato, 1990 and in preparation). The ductile shear zone trends approximately east-west, is estimated at two localities to be approximately 800 to 1,500 m thick, and is traceable along strike for about 13 km (Figure 2). The rocks in this zone are "mylonitic," according to the criteria adopted by Tullis and others (1982): (1) they have undergone grain size reduction, (2) occur in a relatively narrow planar zone, and (3) display enhanced foliation and lineation due to strain concentration.

Field evidence for mylonitization includes a strong south- to southeast-dipping laminar foliation as well as a pronounced southeast-plunging lineation that is defined by aligned mica flakes and stretched quartz and plagioclase feldspar grains. In quartzofeldspathic rocks, comminuted and broken feldspar porphyroclasts are visible on surfaces that expose the XZ plane of the strain ellipsoid. Good examples of such textures are visible in outcrops on Bald Mountain (Stop 10) and can also be seen in Sprignett Creek and in several places in West Fork Evans Creek between Devil's Garden and the confluence with East Fork Evans Creek. Thin sections of rocks cut in the XZ plane commonly display a beautiful fluxion structure. Plagioclase grains are blocky or subrounded and occasionally broken, whereas quartz has deformed ductilely, flowing around the resistant plagioclase grains and forming elongate ribbons up to 5 mm long (Figure 3).

Mylonitic metasedimentary rocks are only locally in direct contact with the underlying amphibolites. The 154-Ma syntectonic diorite is one of several small intrusive bodies emplaced within or near the contact zone, which suggests that the high-temperature shear bands observed within the diorite could also have been formed during mylonitization. Other strongly deformed rocks, including metaserpentinite, Ca-metasomatic rocks, and smaller dioritic intrusive bodies occur within the zone of ductilely deformed rocks. For example, in the West Fork of Evans Creek, mylonitic quartzofeldspathic schist is tectonically interlayered with lenses of sheared metaserpentinite, talc-tremolite schist, thinly layered quartzite, hornblende-biotite schist, hornblende-epidote schist, mylonitic quartzite, gneissic hornblende diorite, and mylonitic amphibolite. The structural thickness of the tectonically disrupted zone at this locality is about 1,500 m. A similar zone of interlayered ultramafic and mafic intrusive rocks separating amphibolite from mylonitic quartzofeldspathic gneisses is exposed in Sprignett Creek. There, the zone is probably only 600-800 m thick.

Oriented thin sections of mylonitic rocks of the May Creek Schist were examined to determine the sense of shear. Kinematic indicators, including S-C fabrics, mica "fish," and rotated tourmaline and plagioclase porphyroblasts in micaceous quartzofeldspathic schist consistently show top-to-the-northwest sense of shear, indicating northwestward transport of the May Creek over amphibolite (Figure 3). In addition, quartz c-axis petrofabric analysis demonstrates top-to-the-northwest sense of shear in eight of 12 localities (the remaining four display strong lattice preferred orientation but cannot be used to interpret sense of shear). Sillimanite occurs with biotite in the deformed micaceous "tails" of an asymmetric rotated tourmaline porphyroblast in a sample also containing quartz, feldspar, and garnet, clearly indicating that metamorphic conditions during the ductile deformation were within the amphibolite facies. This fact, together with the concordance of structures and metamorphic grade between the amphibolite and May Creek and the lack of petrographic evidence for multiple metamorphic episodes, suggests that the north-

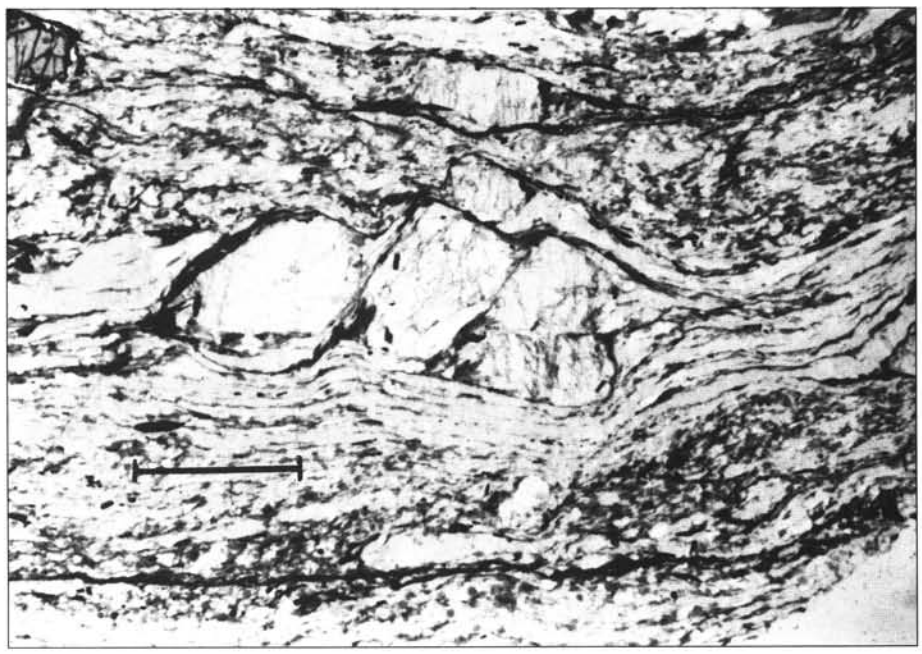

Figure 3. Photomicrograph of broken and rotated plagioclase porphyroblast in mylonitic quartzofeldspathic sample of the May Creek Schist. Three fragments of plagioclase are tilted to the right, indicating dextral sense of shear. Textural evidence such as this together with quartz petrofabric analysis indicates that the May Creek Schist was thrust northwestward over the amphibolite. Biotite and garnet (high-relief mineral in upper left) are also present. Scale bar represents 1 mm.

westward thrusting of the May Creek occurred at the culmination of a single amphibolite-facies metamorphic/deformational event.

SUMMARY

The available petrologic, structural, and geochronologic data for the May Creek Schist, the underlying amphibolite, and associated intrusive rocks allow the construction of a tentative tectonic model for their origin. The geochemistry of the metabasaltic rocks suggests that their protoliths originated in an extensional back-arc basin (Donato, 1991a). These mafic rocks may have formed the oceanic basement upon which clastic sediments, now represented by the May Creek Schist, were deposited. The age of this basin is poorly constrained but must be greater than 154 Ma, the age of the diorite which intrudes the amphibolite. The location of the basin may have been not far from the North American continent, a conclusion based on the abundance of quartz- and feldspar-rich sediments in the lower (older?) parts of the May Creek Schist. Volcanic debris became increasingly abundant as a volcanic arc encroached upon the basin, as represented in the middle and upper parts of the May Creek Schist.

At some time prior to 154 Ma, this basin underwent a compressional event that produced amphibolite-facies metamorphism and folding of the basalts and the overlying sedimentary rocks. Emplacement of serpentinite bodies as tectonic slivers probably occurred at this time. The oldest cooling age thus far obtained from the amphibolite, about 162 Ma, may be a vestige of this event. The 154-Ma diorite must have been emplaced after the inception of this tectonism, because it contains foliated amphibolite xenoliths and produced contact-metamorphic assemblages in adjacent amphibolite; but it could have been partly synchronous with this event, since high-temperature shear bands in the diorite suggest that deformation continued while the intrusion was still hot.

The basin may have collapsed soon after its inception, while the regional heat flow was still high. No obvious localized heat source for amphibolite-facies metamorphism is evident, but if the basin was still young when compression began, temperatures might have been sufficient to account for the high metamorphic grade that is presently seen in the amphibolite and the May Creek Schist and conspicuously absent from the adjacent Rogue and Galice Formations and the Applegate Group. The compression, collapse, and tectonic burial of the still-young and hot basin may have marked its accretion to North America, culminating in the northwestward thrusting of the sedimentary sequence (now called the May Creek Schist) over its igneous (now amphibolitic) basement. This event probably ended during the earliest stages of the so-called Nevadan orogeny in the Klamaths, believed to have lasted from about 155 Ma to 135 Ma (Harper and others, 1989). The 145-Ma and younger cooling ages from the amphibolite suggest that some of these rocks were thermally affected by later so-called Nevadan and younger tectonism and magmatism. The thermal history of this region appears to be complex and bears further investigation.

ACKNOWLEDGMENTS

This paper benefitted from helpful reviews by Russ Evarts and Lynne Fahlquist. Bob Murray recorded mileages, took notes, and provided good company during the construction of the road log.

REFERENCES CITED

Diller J.S., and Kay, G.F., 1924, Description of the Riddle quadrangle, Oregon: U.S. Geological Survey Geologic Atlas, Folio 218, 8 p., 3 map sheets, scale 1:125,000.

Donato, M.M., 1990, A newly recognized ductile shear zone in the northeastern Klamath Mountains [abs.]: Geological Society of America Abstracts with Programs, v. 22, no. 3, p. 19.

———1991a, Geochemical recognition of a captured back-arc basin metabasaltic complex, southwestern Oregon: Journal of Geology, v. 99, no. 5, p. 711-728.

———1991b, Geologic map showing part of the May Creek Schist and related rocks, Jackson County, Oregon: U.S. Geological Survey Miscellaneous Field Studies Map MF-2171, 10 p., map scale 1:62,500.

———in preparation, A newly-recognized ductile shear zone in the northern Klamath Mountains—Implications for Nevadan accretion: U.S. Geological Survey Bulletin.

Harper, G.D., Saleeby, J.B., Pessagno, E.A., Jr., and Heizler, M., 1989, The Josephine ophiolite: generation, translation, and emplacement of a Late Jurassic parautochthonous back-arc lithosphere, Klamath Mountains, California-Oregon [abs.]: Geological Society of America Abstracts with Programs, v. 21, no. 6., p. A28.

Hotz, P.E., 1971, Plutonic rocks of the Klamath Mountains, California and Oregon: U.S. Geological Survey Professional Paper 684-B, 20 p.

Irwin, W.P., 1966, Geology of the Klamath Mountains province, *in* Bailey, E.H., ed., Geology of northern California: California Division of Mines and Geology Bulletin 190, p. 19-38.

Saleeby, J.B., 1984, Pb/U zircon ages from the Rogue River area, western Jurassic belt, Klamath Mountains, Oregon [abs.]: Geological Society of America Abstracts with Programs, v. 16, no. 5, p. 331.

Smith, J.G., Page, N.J., Johnson, M.G., Moring, B.C., and Gray, F., 1982, Preliminary geologic map of the Medford 1° by 2° quadrangle, Oregon and California: U.S. Geological Survey Open File Report 82-955, scale 1:250,000.

Tullis, J., Snoke, A.W., and Todd, V.R., 1982, Significance and petrogenesis of mylonitic rocks (Penrose Conference report): Geology, v. 10, no. 5, p. 227-230.

ROAD LOG—DAY 1, PART 2, RED MOUNTAIN TO BALD MOUNTAIN

Begin in sec. 26, T. 32 S., R. 3 W., southeast corner of the Cedar Springs Mountain 7½-minute quadrangle, at the intersection of National Forest Road (NFD) 230 and NFD 3242. The mileage between points is followed by cumulative mileage in parentheses.

Milepoint 0.0 (0.0)—Start. Quarry in serpentinite. If travelling down from Red Mountain, make a sharp left turn at the intersection and proceed south on NFD 3242. This road becomes BLM Road 33-3-12.2.

1.3 (1.3)—Umpqua National Forest boundary (leaving National Forest). Enter Skeleton Mountain 7½-minute quadrangle.

1.6 (2.9)—Intersection. Take Road 33-3-12.1 eastward (**NOT** southward!). Enter Cleveland Ridge 7½-minute quadrangle.

0.6 (3.5)—Intersection. Bear right on Road 33-2-7.2 and proceed downhill.

2.0 (5.5)—Road 33-2-7.2 meets the Wolf Creek Road (33-2-17). Make a sharp left turn and proceed downhill past many good road cuts in amphibolite.

1.5 (7.0)—Old borrow pit in amphibolite on right. Bridge across the East Fork of Evans Creek.

0.2 (7.2)—Intersection with East Fork Evans Creek Road (33-2-33). Turn left.

1.5 (8.7)—Stop 6. Quarry in amphibolite. This terraced rock quarry has good exposures of metabasites displaying a variety of relict igneous textures visible both in place and in boulders that were blasted from the quarry walls. One can see examples of relict porphyritic textures and intrusive contacts of what may have been sills or dikes. Because many of the rocks are massive and appear to have little directional fabric, they closely resemble fine-grained mafic intrusive rocks. Locally developed hornblende lineation and foliation and textures observed in thin section confirm that these are

in fact amphibolite-facies meta-igneous rocks. They contain hornblende, plagioclase, and sphene or rutile.

Turn around and proceed south on East Fork Evans Creek Road.

1.4 (10.1)—Intersection with Road 33-2-17. Continue straight on East Fork Evans Creek Road.

0.7 (10.8)—Tectonic slivers of talc schist within amphibolite are present in road cuts on the left.

1.7 (12.5)—Stop 7. Near the confluence of the East Fork Evans Creek and Coal Creek. Park in the turnout on the right side of the road just after crossing culvert. Cross the East Fork Evans Creek (carefully, since rocks may be wet and slippery) to see good three-dimensional creekside exposures of interlayered fine- and coarse-grained amphibolite with relict igneous textures. Contacts between "porphyritic" and "aphanitic" varieties are sharp and concordant with the foliation. Some relict plagioclase "phenocrysts" are more than 1 cm long. Outcrop contains felsic veins and segregations, some of which are concordant with the foliation; others are ptygmatically folded. Look closely for small-scale crinkle folds of the foliation.

1.3 (13.8)—Intersection with BLM Road 33-2-33.4. Stay on and continue downhill on East Fork Evans Creek Road. The road crosses the (high-angle?) fault zone marking the contact between amphibolite and Tertiary volcanic and volcaniclastic rocks in this area.

0.1 (13.9)—Sheared and altered Tertiary volcanic rocks.

0.5 (14.4)—Intersection of East Fork Evans Creek Road and road along Chapman Creek. Continue southward on East Fork Evans Creek Road.

0.9 (15.3)—Morrison Creek Road merges from the right with East Fork Evans Creek Road. Continue southward on East Fork Evans Creek Road. In about 1.3 mi, enter Boswell Mountain 7½-minute quadrangle.

3.7 (19.0)—Intersection. Turn right (west), continuing on East Fork Evans Creek Road.

1.3 (20.3)—Stop 8. Park on the right-hand shoulder, completely off the road. This is a narrow, curvy road, so please watch out for traffic. Walk ahead about 0.2 mi to road cuts in quartzite of the May Creek Schist. Since the last stop, we have crossed southward from amphibolite into the structurally higher May Creek Schist, here ranging from foliated quartz-biotite-feldspar-garnet schist to massive, ringing quartzite. Orange-pink color of garnets reflects their Mn- and Ca-rich composition. Quartz in massive quartzite has undulose extinction, but most rocks here are relatively weakly deformed and do not display the mylonitic textures seen elsewhere in the basal part of the May Creek Schist.

0.8 (21.1)—Sprignett Creek Road (34-2-18). This road leads generally northward up a hillside and to a saddle, through many good road cuts in ductilely deformed rocks of the May Creek Schist, metaserpentinite, and amphibolite. This is a good route by which to traverse the ductile shear zone that marks the contact between the amphibolite and the May Creek Schist.

0.8 (21.9)—Entering Skeleton Mountain 7½-minute quadrangle.

0.8 (22.7)—Intersection with West Fork Evans Creek Road (34-3-24). Turn right and proceed upstream. Road cuts on right side of road are quartzites and quartz-mica schists of the May Creek Schist. (Note that some land along the creek is privately owned and is clearly posted "No Trespassing." Please respect the rights of property owners in this area).

0.9 (23.6)—Large parking area on left side of road is the site of a former County maintenance station. There is a path leading down to Evans Creek, where outcrops of folded, well-lineated quartz-mica schist can be seen. By walking downstream, one can also see tectonic slivers of sheared and metasomatized ultramafic rocks interlayered with strongly deformed metasedimentary rocks.

1.0 (24.6)—Stop 9. Bridge over the West Fork Evans Creek. Park on wide shoulder on west (left) side of road and south side of bridge. (Look ahead for oncoming traffic before you make this turn.) Excellent exposures of fresh syntectonic hornblende diorite can be seen across the road in the prominent road cut and, if the water is not too high, in creekbed exposures just beneath and upstream from the bridge. Road cut exposures are massive to locally foliated and lineated, medium- to coarse-grained hornblende diorite containing brown hornblende (with rare clinopyroxene cores), plagioclase, Fe-Ti oxide, and abundant sphene. Look for pegmatitic segregations and felsic veinlets containing small amounts of garnet. Also note thin (1-2 cm) shear bands consisting of fine-grained hornblende and plagioclase. Fine polygonal textures in these narrow bands suggest recrystallization during hot ductile flow. This diorite body appears to concordantly intrude amphibolite: xenoliths of amphibolite are found in outcrops of diorite beneath the bridge. Contact-metamorphosed amphibolite containing diopside + garnet + green spinel + chlorite + clinozoisite + minor calcite crops out high on the creek bank. The extent of the diorite body is difficult to map because of the strong similarities in structure and mineralogy of host and intrusive, but similar small concordant diorite bodies have been noted elsewhere in the amphibolite. A Pb/U age determination on zircon from this locality indicates an intrusive age of approximately 154 Ma, and $^{40}Ar/^{39}Ar$ incremental heating experiments give a cooling age of about 153 Ma.

Continue north on West Fork Evans Creek Road.

0.5 (25.1)—Intersection. Turn left onto Raspberry Creek Road (BLM Road 34-3-15.2) and begin the climb to Bald Mountain.

0.6 (25.7)—Intersection with BLM Road 34-3-15.3. Stay on 34-3-15.2 by bearing left.

0.9 (26.6)—Road cuts in serpentinite and associated amphibolite on the right.

0.7 (27.3)—Intersection with BLM Road 34-3-16.2. Bear right.

1.6 (28.9)—Intersection with BLM Road 34-3-17. Turn left and proceed to the top of Bald Mountain.

2.4 (31.3)—Stop 10. Top of Bald Mountain. This locality provides excellent vistas of the surrounding countryside as well as outstanding outcrops of mylonitic micaceous schist. Park at the end of the road and walk westward on the bulldozed track another hundred feet or so along the crest of the ridge. Then turn northward and descend a short distance down the steep, grassy, north-facing slope to find the outcrops. Quartz-plagioclase-biotite schist here displays typical mylonitic textures: reduction in grain size, enhanced lineation defined by elongated quartz grains, flattened and elongated feldspar grains, and strong foliation. The lineation plunges gently to the southeast. Look in faces parallel to the lineation (the XZ plane of the strain ellipsoid) to find rotated feldspar porphyroclasts that might indicate sense of shear. Thin-section and quartz petrofabric work demonstrates top-to-

the-northwest sense of shear, but this may be difficult to see in outcrop. Also note isoclinal folds that deform foliation.

Turn around and begin descending.

2.5 (33.8)—Intersection with Raspberry Creek Road. Instead of turning right (the way you came), continue straight on Road 34-3-17.

0.7 (34.5)—Quarry in serpentinite. Strongly sheared serpentinite consists mainly of antigorite. This is one of many small serpentinite bodies present near and within the contact zone between the May Creek Schist and the amphibolite. Road cuts just west of the quarry entrance are amphibolite and for the next mile or so alternate between metasedimentary rocks and amphibolite.

0.9 (35.4)—Intersection with May Creek Road (BLM Road 35-3-5). Turn left.

0.5 (35.9)—Road cuts in ultramafic schist and folded amphibolite.

2.5 (38.4)—Confluence of Fawn and May Creeks. A fire devastated this area in 1987 and temporarily made it easier for geologists to see outcrops of the May Creek Schist at its type locality (but watch out for poison oak). Outcrops in the creek consist of monotonous, gray, lineated micaceous quartzite.

0.3 (38.7)—Fawn Creek Road.

1.1 (39.8)—Intersection with Evans Creek Road. Turn right.

1.9 (41.7)—Borrow pit in lineated and foliated rocks of the May Creek Schist on right.

0.3 (42.0)—Road cuts in the May Creek Schist on right.

0.7 (42.7)—Sykes Creek Road.

1.6 (44.3)—Entering town of Wimer. Turn left to cross Wimer Covered Bridge.

0.9 (45.2)—Intersection of Covered Bridge Road with Pleasant Creek Road. Turn left.

3.4 (48.6)—Borrow pit in weathered dioritic rocks of the Wimer pluton.

3.6 (52.2)—Entering town of Rogue River. **End of road log.**

Part 3 (Day 2) of this field trip has been discussed and published elsewhere: See Harper (1989) in references for part 1 on page 32 of this issue. □

TIC invites sponsorship of geologic markers

The Travel Information Council (TIC) is responsible through its historical marker program for commemorating significant events in Oregon. Over 80 sites important to the state's past—from those dealing with glaciation occurring many years ago to the Tillamook Burn from the 1930s—are the subjects of markers. The Department of Geology and Mineral Industries has plans to place at least one new marker per year to highlight and explain the spectacular geologic offerings in Oregon.

The historical marker program began in 1939 and was administered by the Oregon Department of Transportation until July 1991, when it was adopted by TIC. Reactivating a program that was dormant for over 20 years, TIC will refurbish the existing markers and erect new markers throughout the state.

Wallowa Lake marker near Joseph.

A state agency that deals with motorist services, TIC encourages the participation of sponsoring groups in the marker program. New marker application forms ask sponsoring groups to identify the significance of the event, person, or place to be commemorated and to suggest a possible location. Approval of the subject is followed by text and marker design and finally by the manufacture and placement of the marker. In financing the marker, TIC covers 75 percent of the cost; 25 percent is the responsibility of the sponsoring group. Applications can be obtained from the Travel Information Council, 229 Madrona Avenue S., Salem, OR 97302. *—TIC news release*

Capitol mineral display shows new collection

The Clackamette Mineral and Gem Corporation of Oregon City has provided the new exhibit in the display case of the Oregon Council of Rock and Mineral Clubs (OCRMC) at the State Capitol in Salem. It is the first display presented by this club.

Club members Bernie and Winnie Schulz and Jack and Pat Jordan arranged the exhibit on the glass shelves of the 11-ft-long, lighted case. The variety of materials to be found in Oregon is the main theme of the display that shows treasures from 18 Oregon counties, including Thundereggs, Oregon's state rock, and Oregon sunstone, the state gemstone. The collection also presents petrified wood, coral, Tempskya fern, and vertebrae; white and Cedar Mountain jade; rhodonite; jasper from Hart Mountain, Owyhee, and Biggs locations; pink and green limb casts from Crook County; obsidian in slab and sphere forms; Graveyard Point and Eagle Rock plume agate; sagenite; and Holley blue agate from Linn County.

The top shelf features a gem tree made of Oregon sunstones, along with faceted and colored sunstones and two faceted-sunstone necklaces. The shelf below shows a gem tree of Holley blue agate and two framed pictures made with Holley blue agate chips.

The OCRMC display case is located on the main floor of the Capitol building in Salem, in a hall to the west of the information desk. Since it was first installed in 1982, it has held displays by many different Oregon rock clubs. Generally, three displays per year are presented. The new display is scheduled to remain in place until May 15, 1992. *—OCRMC news release*

How geologists tell time—Part 2: Absolute dating techniques

by Evelyn M. VandenDolder, Editor, Arizona Geological Survey.

The following article was originally published as a two-part article in the winter 1990 and spring 1991 issues (v. 20, no. 4; v. 21, no. 1) of *Arizona Geology*, published by the Arizona Geological Survey, 845 N. Park Avenue, Suite 100, Tucson, AZ 85719. With the publisher's permission, Part 1 was reprinted in the November 1991 issue (v. 53, no. 6) of *Oregon Geology*, and Part 2 is reprinted here. In a few cases, the original illustrations had to be replaced with other, similar illustrations. —*Editors*

INTRODUCTION

Geologic time, a revolutionary concept that has taken several centuries to develop, may be measured by both relative and absolute dating techniques. The former were discussed in Part 1 of this article. Nature records earthly time by two absolute methods: astronomically through tree rings, growth rings, and varve sequences, which reflect the rotation and revolution of the Earth in seasonal changes; and atomically through radioactive decay. These two standards of measurement are discussed below.

TREE RINGS

Tree rings are the most familiar seasonal records preserved in living organisms. The width and density of the rings depend on the temperature and the amount of light and moisture present when the plant cells were formed. During the spring and summer growing season, new layers of cells are produced underneath the bark of the tree. Seasonal variations are evident in early or "spring" wood, which consists of large, thin-walled cells, and late or "summer" wood, which consists of smaller cells with thicker walls. One annual ring includes one layer each of spring and summer wood (Figure 1).

Dendrochronology, the study of tree rings, has been used to date archaelogical sites, especially in the arid Southwest, where wooden beams that supported ancient dwellings are well preserved. In living trees, the outer ring was formed during the current year. By counting the total number of rings, scientists can establish an age for the living tree (Figure 2). Because living trees in the same area share a common environment, their rings exhibit a similar pattern of wide and narrow bands, which usually reflect when rainfall was plentiful or scarce, respectively. If the inner-ring pattern of a living tree matches the outer-ring pattern of an ancient tree (e.g., a structural beam of an old building) that grew in the same area, the rings were formed during the same time and, thus, are the same age. Through such cross-dating, dendrochronologists can determine when the ancient tree was cut and the edifice built.

In the Southwest, the continuous tree-ring chronology extends back to 322 B.C. By piecing together tree-ring data from various parts of the world, scientists have extended the continuous chronology even further to 7938 B.C. (Stuiver, 1990). Bristlecone pines in the western United States and oaks in Irish peat bogs are among the trees used to establish this chronology.

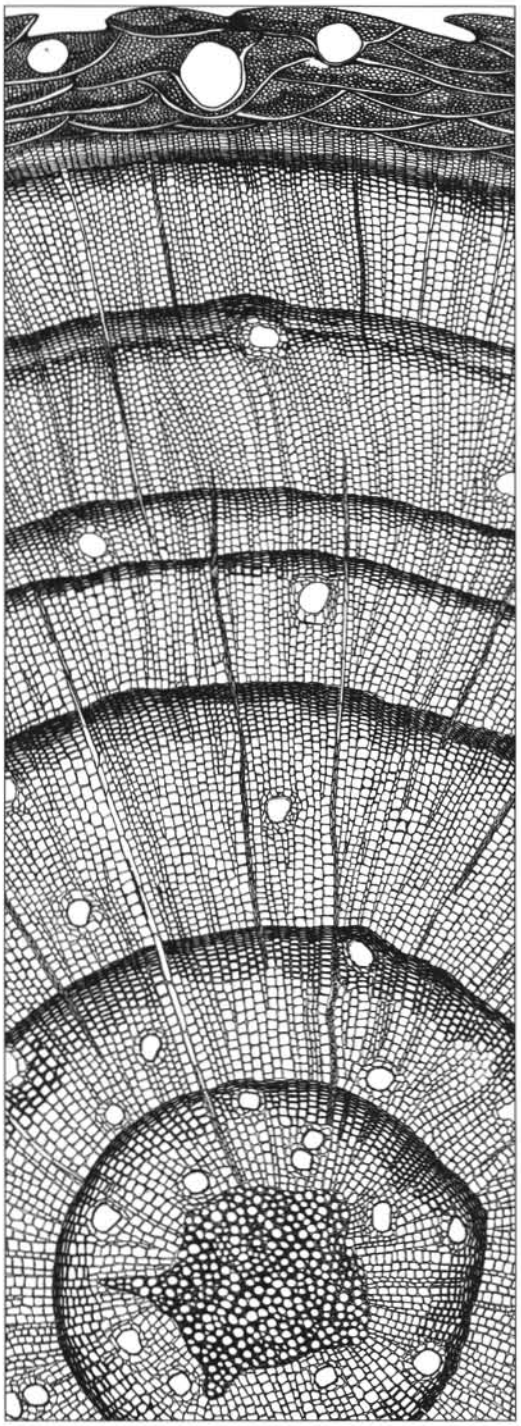

Figure 1 (right). Generalized illustration of the cross-section anatomy of conifers. Note the differences between early or "spring" wood (with large, thin, light-colored cells) and late or "summer" wood (with small, thick, dark-colored cells). New tree rings are produced by the cambrium, a layer of undifferentiated plant cells directly underneath the bark. The large, open circular areas are resin ducts, which are intercellular spaces lined with thin-walled cells that secrete resin into the duct. Resin protects the plant from attack by decay-producing fungi and bark beetles. Drawing by Terah L. Smiley. Copyright 1947 by Laboratory of Tree-Ring Research, University of Arizona. Reprinted with permission.

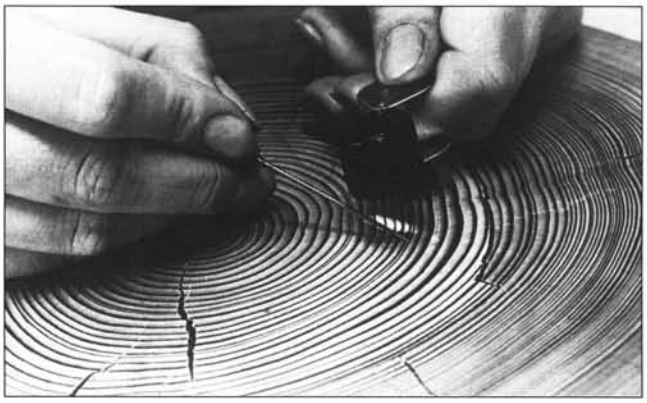

Figure 2. Dendrochronologist examines a cross section of a Douglas fir tree from an archaeological site. Copyright 1984 by Laboratory of Tree-Ring Research, University of Arizona. Reprinted with permission.

GROWTH RINGS

Some aquatic organisms also record seasonal variations in temperature and food supply, especially those that live in lakes in the Temperate Zone where temperature fluctuations are extreme. Freshwater clams typically grow annual bands that resemble tree rings. Dark, narrow bands indicate colder weather, when scarce food restricted shell growth. Lighter and wider bands indicate a warmer season and more abundant food supply (Stokes, 1966). These rings are also evident in fossil shells.

Fish scales, both modern and fossilized, show tiny annual growth rings called "annuli." Corals, on the other hand, record daily growth rings. By studying the rings of fossil corals from the Devonian Period (about 375 million years [m.y.] ago), geologists concluded that there were 400 days in a year and inferred that days were shorter during this time (Stokes, 1966).

VARVE SEQUENCES

Seasonal changes are also reflected in the sedimentary record. Precipitational variations during the wet and dry seasons locally affect erosion, transportation, and deposition of sediments. Wet seasons with high stream flow cause rapid deposition of sediments, whereas dry seasons with low flows cause little or no deposition.

A **varve** is a sedimentary layer deposited in a body of still water, such as a lake, within a single year. The term "varve" specifically refers to an annual layer deposited in a glacial lake by meltwater streams. A glacial varve includes two layers: a lower "summer" layer composed of coarse-grained, light-colored sediments, such as sand or silt, and formed by rapid melting of ice and vigorous runoff during the warmer months; and an upper, thinner "winter" layer composed of very fine grained, often organic, darker clay sediments and produced when suspended particles were slowly deposited while the streams were icebound and the lakes quiet. Glacial varves range from less than an inch to several inches in thickness (Figure 3; Stokes, 1966).

Hundreds of years have been recorded within the varves of a single lake or pond (Stokes, 1966). Variations in the size of varves, due to differences in the length and warmth of seasons, allow geologists to correlate varve sequences. The oldest preserved sequence associated with a particular glacier generally lies adjacent to the area where that glacier reached its maximum extent. The youngest sequence is nearest the glacier's edge (if the glacier still exists) or lies where an "extinct" glacier retreated and melted away. Geologists have counted and correlated varves to determine the ages of Pleistocene glacial deposits and the time when the last ice sheets retreated from Europe and North America.

Figure 3. Middle Pleistocene varves of the Hayden Creek glaciation (approximately 140,000 years B.P.) along Canyon Creek, southeast of the Yale Reservoir, south of Mount St. Helens, Washington. Photo courtesy of Patrick Pringle, Washington Division of Geology and Earth Resources.

RADIOACTIVE DECAY

The nucleus of an atom contains two kinds of particles, each with a mass of 1 (in atomic mass units): **neutrons**, which are electrically neutral, and **protons**, each of which has an electrical charge of +1. The atomic number is equal to the number of protons, which uniquely defines an element and establishes its place among the 103 known elements on the periodic table of the chemical elements. The number of protons is also equal to the number of electrons that surround the nucleus in nonionized atoms. An **electron** has an electrical charge of –1. Because the mass of an electron is negligible, an element's atomic weight essentially equals the total number of protons and neutrons in its nucleus.

Each element consists of several **isotopes**—a word derived from a Greek term meaning "same place" (Faure, 1977). Isotopes have the same number of protons (and thus occupy the "same place" on the periodic table) but different numbers of neutrons (and thus different atomic masses and weights).

Some isotopes of every chemical element are unstable and spontaneously disintegrate to form atoms of different elements, releasing energy in the process. Isotopes radioactively decay through one of three nuclear processes: by emitting **alpha particles**, which are essentially helium nuclei composed of two protons and two neutrons; by emitting **beta particles**, or high-energy electrons; or by capturing electrons. An element that emits an alpha particle becomes another element because it loses two protons. The electrons that are beta particles are not released from the electron cloud surrounding the nucleus but from the nucleus itself.

A neutron breaks up, emits an electron, and becomes a proton, thus creating a new element with one more proton and one less neutron than the previous element. In **electron capture**, a proton in the nucleus picks up an orbital electron and turns into a neutron, thus creating a new element with one less proton and one more neutron (Faure, 1977).

The initial atoms of a radioactive isotope are called **parents**; the new atoms produced after a decay are called **daughters**. One daughter atom is produced by the decay of one parent atom; thus, the number of daughter atoms in a rock or mineral is equal to the number of parent atoms that decayed, as long as no daughter atoms leaked from the sample. Radiometric dating based on the disintegration of parent atoms into daughter atoms may be roughly compared to an hour glass, which tells time by the amount of sand that flows from one chamber to another. By determining the ratio of daughter atoms to parent atoms still in the sample, scientists can determine the original amount of parent atoms in the rock or mineral. For other isotopes, this date represents the time when a mineral cooled to its **blocking temperature**. When the temperature of a mineral is above its blocking temperature, parent or daughter atoms can leak from the sample, thus resetting the radiometric clock or preventing it from even starting. The blocking temperature is specific to the type of mineral. Some geologists study the cooling histories of rocks by determining the radiometric ages of various minerals for which the blocking temperatures are known. This type of research is called **thermochronology**.

The nuclear reactions within radioactive isotopes (also called **radioisotopes**) occur almost instantaneously. Although it is impossible to predict when atoms will disintegrate, scientists have determined how long it takes for a specific quantity of atoms to decay. This rate of decay is determined by the number of atoms (n) that disintegrate in a specific period of time, usually per second or per year, relative to the total number of atoms (N) of that isotope in any given amount of material. The ratio n/N, called the **decay or disintegration constant**, is invariable no matter what N is (Press and Siever, 1982). In other words, the rate of decay is fixed for a given isotope.

Rates of decay, which have been experimentally determined for most radioisotopes, are defined in terms of half-lives. The **half-life** of an isotope is the time required for half of the original number of atoms (parents) to decay. The remaining parent atoms disintegrate at the same rate, being diminished by half during each half-life period until their number approaches zero. [Thus, from one half-life period to the next, the decay proceeds exponentially, e.g., 1—½—¼—⅛, etc., whereas a linear process would appear as 1—½—0. (Illustration of original text not reprinted. -Ed.)] Half-lives range from a fraction of a second in some isotopes to billions of years in others. ^{14}C (pronounced "carbon 14"), a radioisotope of carbon, for example, has a half-life of 5,730 years, whereas ^{87}Rb, a radioisotope of rubidium, has a half-life of 50 billion years (b.y.). The half-life of a radioisotope determines the number of years, and thus the types of rocks or minerals, that it might effectively date. A sophisticated ^{14}C-counting instrument at the University of Arizona in Tucson uses this radioisotope to date objects up to 60,000 years old, or about 10.5 half-lives, at which point only $1/1{,}448$ of the original amount of ^{14}C remains in the sample (P.E. Damon, oral communication, 1991). ^{87}Rb, in contrast, may be used to date the oldest rocks on Earth, which are almost 4 b.y. old.

When dating rocks and minerals by radiometric methods, geologists make three major assumptions. First, the rate of decay is accurately known and constant, i.e., it does not vary with changes in temperature or pressure. Once a quantity of a radioisotope is formed in any part of the universe, it begins releasing atoms at a definite rate. Evidence that decay rates are constant is derived from interpretations of the light spectra of stars, some of which are older than the Earth. Second, the daughter atoms are solely the product of radioactive decay of the parent. No daughter atoms were present in the rock or mineral specimen before the radiometric clock began ticking. Third, the rock or mineral being dated has remained a "closed" system. No changes have occurred, such as reheating, that have allowed daughter atoms to leak out or parent atoms to be added. Such changes would reset the radiometric clock, as would a cracked hourglass that allowed sand grains to escape. Radiometric dating actually determines the time that has elapsed since sand grains escaped from the hourglass, i.e., since the last time that the mineral within a rock sample was at a temperature above its blocking temperature (Faure, 1977).

To count the atoms of a radioisotope, scientists use a **mass spectrometer**, a machine that was developed during the 1920's and 1930's. A mass spectrometer produces a beam of electrically charged atoms from a rock or mineral sample. This beam is then deflected by electrical and magnetic fields. The atoms that compose the beam are proportionately deflected according to their atomic masses, and thus may be separated and counted. During World War II, dating techniques were developed and refined as part of the Manhattan Project, the U.S. government's effort to develop the atomic bomb (Press and Siever, 1982). The mass spectrometer has since evolved into a tool that is used to research problems in geology, chemistry, and biology, as well as physics. Scientists continue to improve the sensitivity and precision of this instrument.

Several radiometric dating techniques are used today. The most common are the K-Ar, Ar-Ar, U-Pb, Th-Pb, Rb-Sr, ^{14}C, and fission-track methods.

K-Ar and Ar-Ar methods

Potassium (K) is one of the eight most abundant elements in the Earth's crust and a major constituent of many rock-forming minerals (Faure, 1977). Because of potassium's abundance and isotopic character, the most commonly used radiometric technique is based on the decay of radioactive potassium (^{40}K).

^{40}K decays via one of two paths: About 89 percent of ^{40}K atoms disintegrates by beta decay to stable calcium (^{40}Ca); the remaining 11 percent disintegrates by electron capture to stable argon (^{40}Ar; Faure, 1977). The quantity of the latter is used to determine the age of the mineral because ^{40}Ar can be distinguished from atmospheric argon, whereas ^{40}Ca cannot be separated from ordinary calcium. In addition, argon can be completely liberated simply by melting the rock or mineral. The K-Ar technique, discovered in 1948 (Stokes, 1966), is used to date potassium-bearing minerals and rocks that retain radiogenic argon at low temperatures. These include biotite and muscovite (both micas) and hornblende in plutonic and metamorphic rocks, as well as feldspar in volcanic rocks. Because they are very common in igneous and metamorphic rocks, micas are the best minerals to date by this technique. The K-Ar method cannot, however, be used to date sedimentary rocks. Minerals that were transported and deposited are generally older than the sedimentary rocks that contain them, and minerals that did form at the same time as the rocks are commonly affected by **diagenesis** (the chemical, physical, and biological processes that turn sediments into rock). The half-life of ^{40}K is 1.31 b.y. Rocks from 10,000 years old to the oldest rocks on Earth may be dated by the K-Ar method (Table 1; Jones, undated).

When using this method to determine the age of crystallization, geologists assume that no argon was present in the mineral when it formed and that it has retained argon since it cooled through its argon blocking temperature (Faure, 1977). ^{40}Ar, however, is the only isotope commonly used in dating that is a gas; thus, it may easily escape from a mineral, especially at temperatures exceeding several hundred degrees centigrade (Dalrymple and Lanphere, 1969). The K-Ar date is the time at which the mineral cooled enough to prevent ^{40}Ar from escaping. This blocking or closure temperature differs with each mineral. For hornblende, for example, the ^{40}Ar blocking temperature ranges between 480 °C and 570 °C, depending on whether the rock cooled slowly (5 °C/m.y.) or quickly (1,000 °C/m.y.). For the feldspar microcline, however, the ^{40}Ar blocking temperature ranges from

Table 1. *Common radiometric dating methods. Compiled from Wyllie (1971), Faure (1977), and Jones (undated)*

Parent	Daughter	Half-life (years)	Effective dating range	Some materials that may be dated
^{40}K	^{40}Ar	1.31 x 10^9	10^4 years to Earth formation	Micas, hornblende, feldspar
^{235}U	^{207}Pb	7.13 x 10^8	10^7 years to Earth formation	Zircon, uraninite, allanite, monazite, sphene, apatite, epidote, thorite
^{238}U	^{206}Pb	4.51 x 10^9	10^7 years to Earth formation	Same as ^{235}U
^{232}Th	^{208}Pb	1.39 x 10^{10}	10^7 years to Earth formation	Same as ^{235}U
^{87}Rb	^{87}Sr	5.0 x 10^{10}	10^7 years to Earth formation	Potassium feldspar, micas, clay minerals
^{14}C	^{14}N	5.73 x 10^3	0 to 6 x 10^4 years	Wood, fabric, paper, rope, seeds, bone, pottery
Fission tracks from U decay			0 years to Earth formation	Apatite, micas, sphene, epidote, garnet, zircon, tektites, glass

120 °C to 180 °C (McDougall and Harrison, 1988). Though perceived as a disadvantage by some scientists, the potential for argon loss is actually considered an advantage by others because K-Ar dates are useful in determining the cooling histories of plutonic and metamorphic rocks.

A variation of the K-Ar technique has been used to overcome some of its limitations. In the Ar-Ar method, the isotopic ratios of ^{40}Ar and ^{39}Ar in the sample are determined. ^{39}Ar is produced from ^{39}K through a reaction induced by neutron irradiation of the sample in an atomic reactor. Because absolute measurements of potassium and argon concentrations are unnecessary, the Ar-Ar method is used to date very small or valuable samples, such as lunar rocks or meteorites. This technique, unlike the K-Ar method, can commonly determine if argon has been added or lost since the time of crystallization (Faure, 1977).

U-Pb and Th-Pb methods

Uranium (U) and thorium (Th) radioactivity, discovered at the turn of the century, was the first to be used in dating rocks and minerals (Faure, 1977). Because they have similar electron configurations, these two elements also have similar chemical properties and decay schemes. Two radioisotopes of uranium (^{235}U and ^{238}U) and one of thorium (^{232}Th) disintegrate to lead (Pb) through alpha and beta decay. The reactions include chains of radioactive intermediate daughters, but the parents and stable daughters are as follows: $^{235}U \rightarrow {}^{207}Pb$; $^{238}U \rightarrow {}^{206}Pb$; and $^{232}Th \rightarrow {}^{208}Pb$ (Faure, 1977).

Ordinary lead consists of four naturally occurring isotopes: ^{208}Pb, ^{207}Pb, ^{206}Pb, and ^{204}Pb. The first three are radioactive-decay products; ^{204}Pb is nonradiogenic. Any lead that was incorporated into a mineral at the time of crystallization consists of all four isotopes. Scientists assume that the total amount of ^{204}Pb has remained constant since the Earth was formed, whereas the amounts of ^{206}Pb, ^{207}Pb, and ^{208}Pb have steadily increased because of radioactive decay (Faure, 1977). The amount of ^{204}Pb is therefore used as a stable reference isotope to determine the ratios of the other lead isotopes.

Separate age calculations using the different uranium isotopes are commonly made for a single sample. Coinciding values, called **concordant ages**, represent the time of crystallization. Values that disagree, called **discordant ages**, indicate that parent or daughter atoms, most commonly lead, were gained or lost through thermal metamorphism (heating) or other processes. By examining the results of these analyses, researchers may be able to obtain both the crystallization and metamorphic ages of the mineral.

The half-lives of ^{235}U, ^{238}U, and ^{232}Th are 713 m.y., 4.5 b.y., and 13.9 b.y., respectively. Rocks from approximately 10 m.y. old to the oldest rocks on Earth may be effectively dated by these methods (Table 1). Intermediate parent-daughter sequences of the ^{235}U and ^{238}U decay series have also been used to date minerals between 50,000 and 300,000 years old (Sawkins and others, 1978). One intermediate sequence, the decay of ^{238}U to ^{234}U and ^{230}Th (the half-life of which is 75,000 years) is used to calibrate radiocarbon dates. (See section titled "^{14}C method.")

As molten magma cools and crystallizes, uranium and thorium become concentrated in the more silica-rich components. Granitic igneous rocks thus contain more uranium and thorium than does basalt (Faure, 1977). Uranium and thorium are contained in many minerals, but minerals that are rich in these elements are rare. Only minerals that retain uranium, thorium, their intermediate daughters, and lead may be effectively dated by the U-Pb and Th-Pb methods. Zircon is the best choice for these techniques; other useful minerals are uraninite (pitchblende), allanite, monazite, sphene, apatite, epidote, and thorite. Because these minerals, as well as uranium and thorium, are commonly present in more silicic rocks, this technique is commonly used to date rocks with a high SiO_2 content (Faure, 1977; Jones, undated).

Rb-Sr method

Radioactive rubidium (^{87}Rb), through release of a beta particle, disintegrates to strontium (^{87}Sr). Because the half-life of ^{87}Rb is so long (about 50 b.y.), its accuracy is somewhat uncertain. For this reason, the Rb-Sr method cannot be used to date young rocks.

The Rb-Sr technique is used to date rubidium-bearing minerals, such as micas, potassium feldspar, and clay minerals, in igneous and metamorphic rocks (Table 1). Thermal metamorphism may release daughter atoms and reset the radiometric clock in rubidium-bearing minerals. Whole-rock samples the size of hand specimens, however, may remain closed systems even if metamorphism has occurred (Faure, 1977). Rubidium and strontium may migrate from one mineral to another but remain within the rock. The Rb-Sr technique, therefore, may be used to establish the time of crystallization through whole-rock analysis, as well as the time of metamorphism through separate mineral analyses. It may be the most valuable method for dating metamorphic rocks.

^{14}C method

Radioactive carbon (^{14}C) is naturally created in the atmosphere when cosmic-ray-produced neutrons interact with stable nitrogen (^{14}N) atoms, causing each atom to lose one proton. The ^{14}C atoms are quickly oxidized to CO_2. When a plant is alive, it "breathes" in CO_2 and incorporates into its cell structure carbon molecules from the CO_2 through the process of photosynthesis. Carbon from the atmosphere includes both radioactive ^{14}C and the more abundant stable isotope ^{12}C. When a plant dies, photosynthesis and CO_2 intake both cease. As the age of the dead organic material increases, the amount of ^{14}C in that material decreases due to beta decay to ^{14}N, whereas the amount of ^{12}C does not. The $^{14}C/^{12}C$ ratio in the plant material provides a measure of the time that has elapsed since the organism died (Faure, 1977).

Unlike other radioisotopes, ^{14}C does not have to be measured by use of a mass spectrometer. Instead, the amount of ^{14}C in the sample may be indirectly determined by counting the number of beta particles emitted, which is proportional to the number of ^{14}C atoms present. This total is compared to the ^{14}C radioactivity in living plant tissues. In preparation for ^{14}C dating, the sample is treated to remove impurities and burned with oxygen or treated with acid to release CO_2 gas. This gas is also treated to remove impurities and compressed within a copper tube. ^{14}C emissions are then counted for 12 hours or more, depending on the sample's age (Faure, 1977).

During the past decade, mass spectrometry has been increasingly used instead of radioactive-decay counting to measure minute amounts of ^{14}C. This method allows researchers to count all the ^{14}C atoms in a sample (or at least those that the detector collects), not only those that decay during the counting period (Levi, 1990).

The ^{14}C method is used to date charcoal, wood, fabric, seeds, nutshells, paper, hide, rope, bone, ivory, and pottery, especially for archaeological purposes. The half-life of ^{14}C is about 5,730 years. The most sophisticated mass spectrometers can use ^{14}C to date small samples up to 45,000 years old. The most sophisticated counting instruments can date larger samples up to 60,000 years old (P.E. Damon, oral communication, 1991; Table 1).

The ^{14}C dating technique is based on two assumptions: (1) the level of ^{14}C activity is constant in both the atmosphere and biosphere; it does not vary with time, latitude, or species; and (2) the sample is a closed system; no ^{14}C was incorporated into tissues after the organism's death, and radioactivity is the sole cause of ^{14}C depletion. Researchers have shown, however, that the ^{14}C content of the atmosphere varies with the level of cosmic-ray activity, which in turn depends on latitude, solar activity, and the Earth's magnetic field. About 20,000 years ago, the ^{14}C content of the atmosphere was 40 percent higher than it is today (Levi, 1990). This variation is mainly due to changes in the Earth's magnetic dipole, which 30,00 years ago was only about half its current strength (Levi, 1990). The weaker field allowed more cosmic rays to penetrate the atmosphere at the mid-latitudes and thus generate more ^{14}C.

Variations in atmospheric ^{14}C levels due to human activities have also been noted. ^{14}C levels decreased from the 19th to the 20th century, possibly because of the combustion of fossil fuels during the Industrial Revolution, which added "dead" ^{14}C-depleted CO_2 to the atmosphere. They have risen, however, since 1945 because of the development of the atomic bomb, nuclear reactors, and particle accelerators (Faure, 1977). In addition to fluctuating levels of atmospheric ^{14}C, ^{14}C from surrounding water, soil, rock, or vegetation may contaminate a sample.

Because these variations may affect the accuracy of radiocarbon dates, studies of tree rings and varve sequences are commonly used to check and correct ^{14}C dates of sample materials. By measuring the ^{14}C content of annual rings in bristlecone pines and other trees and of varved sediments that contain organic matter, researchers can determine the ^{14}C content of the atmosphere at the time the rings and varves were formed. Radiocarbon dates that are cross-checked with dates from tree rings or varve sequences are exceptionally accurate. These calibrations, however, cover only about the last 9,000 years of Earth history (Levi, 1990).

By comparing ^{14}C and $^{230}Th/^{234}U$ ages of submerged Barbados corals researchers have recently shown that radiocarbon dates of 20,000 years could be as much as 3,800 years too young (Bard and others, 1990; Stuiver, 1990). Because the $^{230}Th/^{234}U$ dates were determined by a high-precision mass-spectrometry technique, the researchers were able to calibrate ^{14}C dates up to 40,000 years ago (Levi, 1990). The adjusted ^{14}C time scale recalibrates the dates of global glacial periods, as well as the ages of some archaeological artifacts. Scientists will continue to refine radiocarbon dating techniques and use other methods to cross-check ^{14}C dates.

Fission-track method

Uranium isotopes generally disintegrate by emitting an alpha particle but sometimes undergo an alternate mode of decay: spontaneous nuclear fission. The nucleus spontaneously breaks into two charged particles that travel in opposite directions, leaving trails of molecular destruction as their energy is transferred to the atoms of the mineral. If the mineral is etched with acid, the more soluble damaged areas become enlarged and are visible as tracks under an optical microscope (Figure 4). These tubular **fission tracks**, which are mostly created by the spontaneous fission of ^{238}U atoms, are 2-3 microns wide and 10-20 microns long (Gleadow and others, 1983). Scientists estimate that for every 2 million ^{238}U atoms that decay by alpha emission only one will fission (Jones, undated).

The density of fission tracks in a mineral increases with time and uranium concentration, but the tracks disappear if the mineral is heated above a specific temperature, known as the **annealing temperature**. Tracks in different minerals have different annealing temperatures. The fission-track method can thus provide information about the thermal histories of rocks. A fission-track date is the cooling age, not necessarily the crystallization age, of the mineral. If the mineral cooled rapidly and was not reheated, the date is the actual age of the mineral. The fission-track method is used to date apatite, micas, sphene, epidote, garnet, zircon, tektites, volcanic glass, and synthetic glass, including some archaeological objects (Faure, 1977). Samples from one decade old to the oldest rocks on Earth may be dated by this technique (Table 1; Jones, undated).

To date a mineral by the fission-track method, a researcher must determine both the density of fission tracks and the uranium concentration within the specimen. A fresh, unweathered surface of the mineral is cut, polished, and etched with acid. The specimen is then placed under a petrographic microscope, and the fission tracks are counted within a known area. To determine the uranium concentration of the sample, the researcher may prepare the sample in one of two ways. For minerals, such as apatite, in which the uranium content is homogeneous, i.e., the same in each grain, the spontaneous fission tracks are annealed, or destroyed by heating, after they are counted. The researcher then cuts, polishes, and etches a new surface of the mineral. To date minerals with nonhomogeneous uranium, such as zircon and sphene, the researcher does not heat or etch the mineral. Muscovite containing very little uranium is attached to the sample to serve as a track detector (Faure, 1977; Jones, undated). After preparing the sample by either method, the researcher irradiates it with thermal neutrons in a nuclear reactor to induce fission of ^{235}U atoms and counts the density of induced fission tracks. Because the ratio of ^{238}U to ^{235}U atoms is constant in nature (137.8:1; Faure, 1977), the density of induced ^{235}U fission tracks may be compared with that of spontaneous ^{238}U fission tracks to determine the number of parent atoms that were originally in the sample.

Fission-track dating has several advantages. This analysis does not require the use of a mass spectrometer and is relatively easy to perform. It may be used to date materials, such as highly weathered rocks and minerals, that cannot be dated by other means. Disadvantages of this method, however, are that the track density of the sample must exceed 10 tracks per cm^2 and that the sample must be relatively free of inclusions and defects to permit counting (Faure, 1977).

Alpha particles emitted by radioisotopes do not release enough energy to produce fission tracks. They may, however, produce **pleochroic haloes**, minute, dark or colored concentric rings surrounding inclusions of radioactive minerals. The intensity of the ring color depends on the number of alpha emissions. Coloration increases to a maximum intensity, as the number of emissions and the age of the mineral increase, but then decreases, as radiation damage becomes extreme. Pleochroic haloes have been extensively studied in biotite, because this mineral has perfect cleavage, and the haloes are readily visible. The accuracy of the pleochroic-halo dating method, however, remains controversial (Faure, 1977).

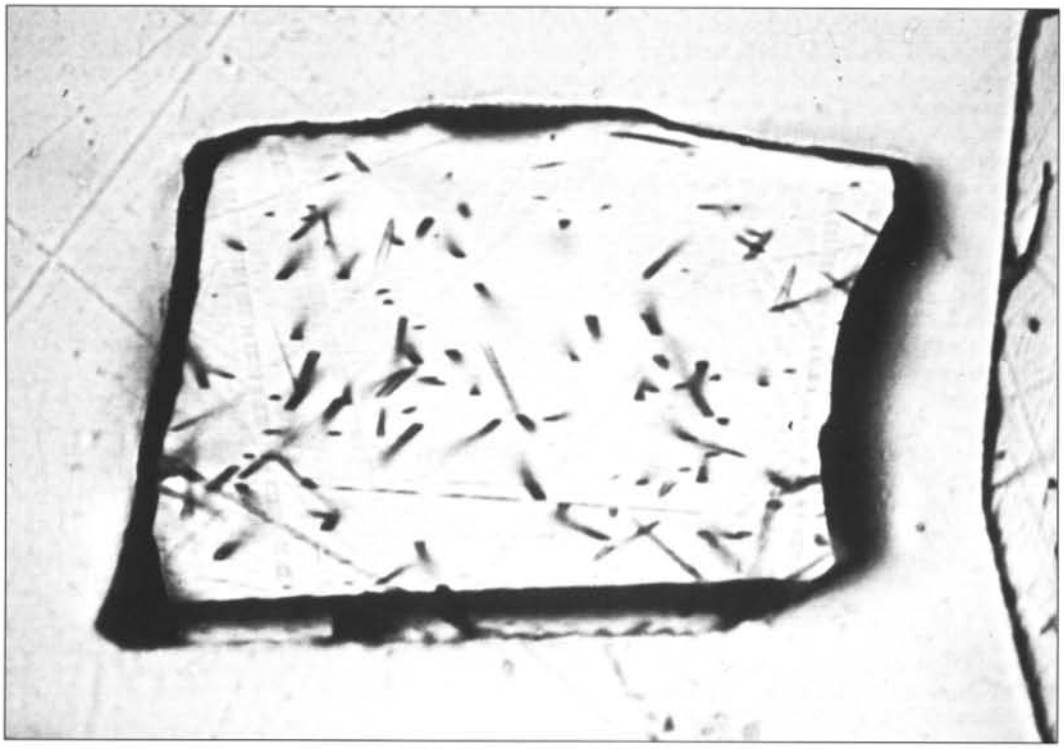

Figure 4. Spontaneous fission tracks in apatite mineral grain, as viewed through a petrographic microscope at a magnification of 1,000X. These natural tracks (short, dark lines) were produced by the spontaneous fission of ^{238}U atoms. The very long, light-colored lines are merely scratches of the surface of the grain. This apatite is from a granodiorite from the Dry Valleys of Antarctica. The apatite fission-track age of this particular sample (58 ± 4 m.y.) reflects early Cenozoic uplift of the Transantarctic Mountains. Photo by Paul Fitzgerald, Department of Geology, Arizona State University.

Other methods

Several other techniques have been used to date certain rocks and minerals that cannot be dated by the conventional methods described above. The most promising methods are based on beta decay of the naturally occurring radioisotopes of rhenium (^{187}Re) and lutetium (^{176}Lu) to osmium (^{187}Os) and hafnium (^{176}Hf), respectively. The Re-Os method is used to date iron meteorites, molybdenite-bearing vein deposits, and rhenium-bearing copper-sulfide ores. The Lu-Hf method is used to date apatite, garnet, and monazite in igneous rocks. The naturally occurring radioisotopes of some rare-earth elements, most notably samarium (^{147}Sm) and lanthanum (^{138}La), have also been used to make age determinations (Faure, 1977). The alpha decay of samarium (^{147}Sm) to neodymium (^{143}Nd) has been used to date Precambrian rocks but is more commonly used as an isotropic tracer to study the genesis and history of the Earth's crust.

Although the radioactive decay of ^{40}K to ^{40}Ar, described above, is more widely used as a dating technique, the decay of ^{40}K to ^{40}Ca may be used to date minerals that are greatly enriched in potassium and depleted in calcium, such as micas in pegmatite and sylvite in evaporite rocks (Faure, 1977). The high natural abundance of ^{40}Ca, however, does pose problems with this method.

Tritium (^{3}H), a radioisotope of hydrogen, is created in the atmosphere from ^{14}N in a way similar to ^{14}C production but in smaller amounts. It is also produced by manmade nuclear explosions. Tritium, which decays to stable Helium (^{3}He), has a short half-life of about 12.5 years (Stokes, 1966; Faure, 1977). It is therefore not used to date geologic events but may be used to determine the flow rate of ground water and the circulation rate of deep ocean currents.

THE IMPORTANCE OF DATING ROCKS AND MINERALS

By dating rocks and minerals, geologists can clarify the chronology of geologic events, relationships between rock units, sources of rock materials, and timing of metamorphic and mineralizing events. Age determinations are so important to geologists deciphering the geologic history of Arizona that more than 1,600 radiometric dates had been determined for rocks in the state by 1986 (Reynolds and others, 1986). Because this history is extremely complex, geologists continue to generate dozens of new radiometric dates each year. Relative dating methods, such as those based on sedimentary sequences, fossils, and cross-cutting relationships, as well as other absolute dating methods, such as those based on tree rings, are no less valuable to geologists. These techniques provide geologic information and insights that radiometric dates cannot offer. They are also crucial to understanding the relationship between radiometric dates and the geologic history of an area. Some examples of the knowledge gained by geochronologic studies in Arizona are given below.

Such studies in western Arizona have helped in understanding the geologic history of the Gulf of California region. The Bouse Formation along the Colorado River consists of estuarine deposits, or sediments deposited in the brackish water of an **estuary**, an arm of the sea at the lower end of a river. Fossils and volcanic tuffs associated with this formation indicate that it is early Pliocene to late Miocene in age. This age and the composition of the formation suggest that the Gulf of California and the Salton Trough were connected 3-11 m.y. ago (Schmidt, 1990).

By dating minerals within a mountain range, geologists can determine not only when the rocks were formed and uplifted but also the rate of the orogenic (mountain-building) process. Rocks in the forerange of the Santa Catalina Mountains near Tucson and in the South Mountains near Phoenix were once thought to be Precambrian, or approximately 1.6 b.y. old. Because of new age determinations, it is now known that the rocks were formed during the Tertiary period. Uplift of these mountains, which was relatively fast (in geologic terms), largely occurred between 30 and 15 m.y. ago.

The mountains in the Basin and Range Province of Arizona are mostly composed of igneous and metamorphic rocks. Many of the granites in these ranges are very similar in appearance and could not be distinguished from each other without knowledge of their ages. By using radioisotopes, geologists can link ore deposits with specific intrusive episodes and formations. Except in the Bisbee area, all porphyry copper deposits in Arizona are associated with granites of a specific age (early Tertiary to Late Cretaceous, or 55-75 m.y. old). Some minerals, such as micas, were formed by the mineralizing process and therefore may be used to date the deposits. By dating micas at the Vulture mine, geologists from the Arizona Geological

Survey (AZGS) and U.S. Geological Survey (USGS) have determined that this deposit is Cretaceous, not Precambrian, as was previously thought (Spencer and others, 1989). Knowing the age of a mineral deposit is important to explorationists who are searching for more deposits of the same type.

Geothermal energy (useful energy that can be harnessed from naturally occurring steam and hot water, such as hot springs, fumaroles, and geysers) is associated with areas of Quaternary volcanic activity. Volcanic rocks in western Arizona were once thought to be Quaternary (less than 1.6 m.y. old) or Cretaceous (66-144 m.y. old). If they had been Quaternary, they would have been prime sites for geothermal energy, and thus they were the subject of several geothermal studies. If they had been Cretaceous, they would have been prime sites for porphyry copper deposits. Because of recent geologic mapping and age determinations by geologists from the AZGS, USGS, and University of Arizona, it is now known that these rocks are middle Tertiary (20-40 m.y. old). Geologists can now link these rocks with other mid-Tertiary volcanic rocks (and hence other episodes of volcanism) in southern Arizona, such as those in the Chiricahua and Superstition Mountains.

By dating Quaternary materials, such as terrace (flood-plain) deposits and sediments that are cut by or overlap faults, geologists can determine the potential for flooding, earthquakes, and other geologic hazards in an area. AZGS geologists have also dated terrace deposits and studied the pattern of erosion along stream channels in the Tucson area. They have established when the last flood occurred and estimated the potential for future floods in the metropolitan area.

As the population of Arizona continues to grow, along with the demand for mineral resources and responsible city planning, the need for reliable geologic mapping, including accurate age determinations of rock units, will become increasingly important.

REFERENCES CITED

Bard, E., Hamelin, B., Fairbanks, R.G., and Zindler, A., 1990, Calibration of the ^{14}C time scale over the past 30,000 years using mass-spectrometric U-Th ages from Barbados corals: Nature, v. 345, p. 405-410.

Dalrymple, G.B., and Lanphere, M.A., 1969, Potassium-argon dating: Principles, techniques, and applications to geochronology: San Francisco, W.H. Freeman and Co., 258 p.

Faure, G., 1977, Principles of isotope geology: New York, John Wiley and Sons, Inc., 464 p.

Gleadow, A.J.W., Duddy, I.R., and Lovering, J.F., 1983, Fission track analysis: A new tool for the evaluation of thermal histories and hydrocarbon potential: Australian Petroleum Exploration Association Journal, v. 23, p. 93-102.

Jones, L.M., undated, The dating game, or an introduction to geochronology: CONOCO, Inc., unpublished manuscript, 59 p.

Levi, B.G., 1990, Uranium-thorium dating sets the clock back on carbon-14 ages: Physics Today, v. 43, no. 9, p. 20-21.

McDougall, I., and Harrison, T.M., 1988, Geochronology and thermochronology by the $^{40}Ar/^{39}Ar$ method: New York, Oxford University Press, 212 p.

Press, F., and Siever, R., 1982, Earth (3d ed.): San Francisco, W.H. Freeman and Co., 613 p.

Reynolds, S.J., Florence, F.P., Welty, J.W., Roddy, M.S., Currier, D.A., Anderson, A.V., and Keith, S.B., 1986, Compilation of radiometric age determinations in Arizona: Arizona Bureau of Geology and Mineral Technology Bulletin 197, 258 p.

Sawkins, F.J., Chase, C.G., Darby, D.G., and Rapp, G., Jr., 1978, The evolving Earth (2d ed.): New York, Macmillan Publishing Co., Inc., 558 p.

Schmidt, N., 1990, Plate tectonics and the Gulf of California region: Arizona Geology, v. 20, no. 2, p. 1-4.

Spencer, J.E., Reynolds, S.J., Grubensky, M.J., Duncan, J.T., and White, D.C., 1989, Geology of the Vulture gold mine: Arizona Geology, v. 19, no. 4, p. 1-4.

Stokes, W.L., 1966, Essentials of Earth history (2d ed.): Englewood Cliffs, N.J., Prentice-Hall, Inc., 468 p.

Stuiver, M., 1990, Timescales and telltale corals: Nature, v. 345, p. 387-388.

Wyllie, P.J., 1971, The dynamic Earth: Textbook in geosciences: New York, John Wiley and Sons, Inc., 416 p. □

Announcement

Annual Pacific Northwest Mining and Metals Conference

MINING, EXPLORATION and the ENVIRONMENT '92

Bellevue, Hyatt Regency Washington April 6-10, 1992

Sponsored by: North Pacific Section of the Society for Mining, Metallurgy and Exploration, with 3 sessions sponsored by the Association of Exploration Geochemists

Preconvention Short courses (April 6-7, 1992)

- Exploration Geochemistry - Dr. Stan J. Hoffman, Prime Geochemical Methods Ltd.
- MagmaChem - Metal Series - Stanley B. Keith, MagmaChem Exploration, Inc.
- Alkalic Systems - Dr. Felix Mutschler, Depart. of Geology, Eastern Washington Univ.
- Wetlands Design for Bioremediation - Dr. John T. Gomley, Knight Piesold and Co.

Technical Sessions (April 8-10, 1992)

- Exploration and the Environment
- Modern Methods of Multi-element Analysis
- Recent Advances in Stream Sediment Geochemistry
- Explo '92 - Exploration Strategies for the 90's
- New Discoveries/Case Histories
- Environmental Considerations for the 90's
- Remediation of Mine Wastes
- Acid Mine Drainage
- Abandoned Mine Lands
- Extractive Metallurgy
- Heap Leach Pad and Tailings Design
- Surface and Underground Mining
- Controversial Geological Concepts

Field Trips

- Coal Country - John Henry Mine and Centralia Mine, Washington
- Cannon Gold Mine, Washington
- Republic-Oroville Gold Country - Hecla-Republic Unit: Echo Bay/Crown Resources; Kettle River Project: Crown Resources/Battle Mountain Gold; Buckhorn/Crown Jewel Project
- Alkalic Porphyry Tour - Southeastern B.C.

Trade Show: 24 booths available

Registration fee: US $85 ($95 for nonmembers and $20 for students) postmarked by February 29, 1992, $110 ($120 and $25) after February 29, 1992.

For more information and registration form, please contact:

Carl Johnson
Science Applications International Corp.
18702 North Creek Parkway, Suite 211
Bothell, Washington 98011
Phone: (206)485-2818
Fax: (206)487-1473

GeoRef offers new serials list

GeoRef, the bibliographic data base produced and maintained by the American Geological Institute (AGI), now offers its latest edition of the *GeoRef Serials List* (1991).

This list contains entries for 11,520 journals and other serial publications that have been or are currently cited in the GeoRef data base. The list includes a main section that lists titles alphabetically and a secondary section arranged by publisher.

GeoRef is the most comprehensive geoscience data base in the world. It is updated monthly with more than 5,000 references. Serials account for roughly 75 percent of the 1.6 million references currently in GeoRef. AGI is a nonprofit federation of 19 member organizations representing geologists, geophysicists, and other earth scientists.

The *GeoRef Serials List* (364 pages, unbound, prepunched) is available for $95 from the AGI Publications Center, P.O. Box 2010, Annapolis Junction, MD 20701. *—AGI news release*

Mabey earns doctoral degree

Matthew A. Mabey, who joined the Oregon Department of Geology and Mineral Industries (DOGAMI) in December 1990 as Earthquake Engineer, successfully completed the oral defense of his dissertation and has earned the degree of Doctor of Philosophy in Civil Engineering from Brigham Young University. The subject of his dissertation research was the assessment of liquefaction as an earthquake hazard, and the title of his dissertation is "Prediction of displacements due to liquefaction-induced lateral spreads."

Mabey earned two undergraduate degrees (B.S. in geology and B.S. in geophysics, 1981) at the University of Utah and a Master of Science degree in civil engineering (1989) at Brigham Young University. In addition to his work with DOGAMI, he teaches classes on earthquake hazards at Portland State University. □

AVAILABLE PUBLICATIONS
OREGON DEPARTMENT OF GEOLOGY AND MINERAL INDUSTRIES

GEOLOGICAL MAP SERIES

		Price	√
GMS-4	Oregon gravity maps, onshore and offshore. 1967	4.00	
GMS-5	Powers 15-minute quadrangle, Coos and Curry Counties. 1971	4.00	
GMS-6	Part of Snake River canyon. 1974	8.00	
GMS-8	Complete Bouguer gravity anomaly map, central Cascade Mountain Range. 1978	4.00	
GMS-9	Total-field aeromagnetic anomaly map, central Cascade Mountain Range. 1978	4.00	
GMS-10	Low- to intermediate-temperature thermal springs and wells in Oregon. 1978	4.00	
GMS-12	Oregon part of the Mineral 15-minute quadrangle, Baker County. 1978	4.00	
GMS-13	Huntington and parts of Olds Ferry 15-minute quadrangles, Baker and Malheur Counties. 1979	4.00	
GMS-14	Index to published geologic mapping in Oregon, 1898-1979. 1981	8.00	
GMS-15	Free-air gravity anomaly map and complete Bouguer gravity anomaly map, north Cascades, Oregon. 1981	4.00	
GMS-16	Free-air gravity and complete Bouguer gravity anomaly maps, southern Cascades, Oregon. 1981	4.00	
GMS-17	Total-field aeromagnetic anomaly map, southern Cascades, Oregon. 1981	4.00	
GMS-18	Rickreall, Salem West, Monmouth, and Sidney 7½-minute quadrangles, Marion and Polk Counties. 1981	6.00	
GMS-19	Bourne 7½-minute quadrangle, Baker County. 1982	6.00	
GMS-20	S½ Burns 15-minute quadrangle, Harney County. 1982	6.00	
GMS-21	Vale East 7½-minute quadrangle, Malheur County. 1982	6.00	
GMS-22	Mount Ireland 7½-minute quadrangle, Baker and Grant Counties. 1982	6.00	
GMS-23	Sheridan 7½-minute quadrangle, Polk and Yamhill Counties. 1982	6.00	
GMS-24	Grand Ronde 7½-minute quadrangle, Polk and Yamhill Counties. 1982	6.00	
GMS-25	Granite 7½-minute quadrangle, Grant County. 1982	6.00	
GMS-26	Residual gravity, northern, central, and southern Oregon Cascades. 1982	6.00	
GMS-27	Geologic and neotectonic evaluation of north-central Oregon. The Dalles 1° x 2° quadrangle. 1982	7.00	
GMS-28	Greenhorn 7½-minute quadrangle, Baker and Grant Counties. 1983	6.00	
GMS-29	NE¼ Bates 15-minute quadrangle, Baker and Grant Counties. 1983	6.00	
GMS-30	SE¼ Pearsoll Peak 15-minute quadrangle, Curry and Josephine Counties. 1984	7.00	
GMS-31	NW¼ Bates 15-minute quadrangle, Grant County. 1984	6.00	
GMS-32	Wilhoit 7½-minute quadrangle, Clackamas and Marion Counties. 1984	5.00	
GMS-33	Scotts Mills 7½-minute quadrangle, Clackamas and Marion Counties. 1984	5.00	
GMS-34	Stayton NE 7½-minute quadrangle, Marion County. 1984	5.00	
GMS-35	SW¼ Bates 15-minute quadrangle, Grant County. 1984	6.00	
GMS-36	Mineral resources of Oregon. 1984	9.00	
GMS-37	Mineral resources, offshore Oregon. 1985	7.00	
GMS-38	NW¼ Cave Junction 15-minute quadrangle, Josephine County. 1986	7.00	
GMS-39	Bibliography and index, ocean floor and continental margin off Oregon. 1986	6.00	
GMS-40	Total-field aeromagnetic anomaly maps, Cascade Mountain Range, northern Oregon. 1985	5.00	
GMS-41	Elkhorn Peak 7½-minute quadrangle, Baker County. 1987	7.00	
GMS-42	Ocean floor off Oregon and adjacent continental margin. 1986	9.00	
GMS-43	Eagle Butte and Gateway 7½-minute quadrangles, Jefferson and Wasco Counties. 1987	5.00	
	as set with GMS-44 and GMS-45	11.00	
GMS-44	Seekseequa Junction and Metolius Bench 7½-minute quadrangles, Jefferson County. 1987	5.00	
	as set with GMS-43 and GMS-45	11.00	
GMS-45	Madras West and Madras East 7½-minute quadrangles, Jefferson County. 1987	5.00	
	as set with GMS-43 and GMS-44	11.00	
GMS-46	Breitenbush River area, Linn and Marion Counties. 1987	7.00	
GMS-47	Crescent Mountain area, Linn County. 1987	7.00	
GMS-48	McKenzie Bridge 15-minute quadrangle, Lane County. 1988	9.00	
GMS-49	Map of Oregon seismicity, 1841-1986. 1987	4.00	
GMS-50	Drake Crossing 7½-minute quadrangle, Marion County. 1986	5.00	
GMS-51	Elk Prairie 7½-minute quadrangle, Marion and Clackamas Counties. 1986	5.00	
GMS-53	Owyhee Ridge 7½-minute quadrangle, Malheur County. 1988	5.00	
GMS-54	Graveyard Point 7½-minute quadrangle, Malheur and Owyhee Counties. 1988	5.00	
GMS-55	Owyhee Dam 7½-minute quadrangle, Malheur County. 1989	5.00	
GMS-56	Adrian 7½-minute quadrangle, Malheur County. 1989	5.00	
GMS-57	Grassy Mountain 7½-minute quadrangle, Malheur County. 1989	5.00	
GMS-58	Double Mountain 7½-minute quadrangle, Malheur County. 1989	5.00	
GMS-59	Lake Oswego 7½-minute quadrangle, Clackamas, Multnomah, and Washington Counties. 1989	7.00	
GMS-61	Mitchell Butte 7½-minute quadrangle, Malheur County. 1990	5.00	
GMS-63	Vines Hill 7½-minute quadrangle, Malheur County. 1991	5.00	
GMS-64	Sheaville 7½-minute quadrangle, Malheur County. 1990	5.00	
GMS-65	Mahogany Gap 7½-minute quadrangle, Malheur County. 1990	5.00	
GMS-67	South Mountain 7½-minute quadrangle, Malheur County. 1991	6.00	
GMS-68	Reston 7½-minute quadrangle, Douglas County. 1990	6.00	
GMS-75	Portland 7½-minute quadrangle, Multnomah, Washington, and Clark Counties. 1991	7.00	

BULLETINS

33	Bibliography of geology and mineral resources of Oregon (1st supplement, 1936-45). 1947	4.00	
35	Geology of the Dallas and Valsetz 15-minute quadrangles, Polk County (map only). Revised 1964	4.00	
36	Papers on Foraminifera from the Tertiary (v. 2 [parts VII-VIII] only). 1949	4.00	
44	Bibliography of geology and mineral resources of Oregon (2nd supplement, 1946-50). 1953	4.00	
46	Ferruginous bauxite, Salem Hills, Marion County. 1956	4.00	
53	Bibliography of geology and mineral resources of Oregon (3rd supplement, 1951-55). 1962	4.00	
61	Gold and silver in Oregon. 1968 (reprint)	20.00	
65	Proceedings of the Andesite Conference. 1969	11.00	
67	Bibliography of geology and mineral resources of Oregon (4th supplement, 1956-60). 1970	4.00	
71	Geology of lava tubes, Bend area, Deschutes County. 1971	6.00	
78	Bibliography of geology and mineral resources of Oregon (5th supplement, 1961-70). 1973	4.00	
81	Environmental geology of Lincoln County. 1973	10.00	
82	Geologic hazards of Bull Run Watershed, Multnomah and Clackamas Counties. 1974	8.00	
87	Environmental geology, western Coos/Douglas Counties. 1975	10.00	
88	Geology and mineral resources, upper Chetco River drainage, Curry and Josephine Counties. 1975	5.00	
89	Geology and mineral resources of Deschutes County. 1976	8.00	
90	Land use geology of western Curry County. 1976	10.00	
91	Geologic hazards of parts of northern Hood River, Wasco, and Sherman Counties. 1977	9.00	
92	Fossils in Oregon. Collection of reprints from the *Ore Bin*. 1977	5.00	
93	Geology, mineral resources, and rock material, Curry County. 1977	8.00	
94	Land use geology, central Jackson County. 1977	10.00	
95	North American ophiolites (IGCP project). 1977	8.00	
96	Magma genesis. AGU Chapman Conf. on Partial Melting. 1977	15.00	
97	Bibliography of geology and mineral resoures of Oregon (6th supplement, 1971-75). 1978	4.00	
98	Geologic hazards, eastern Benton County. 1979	10.00	
99	Geologic hazards of northwestern Clackamas County. 1979	11.00	
100	Geology and mineral resources of Josephine County. 1979	10.00	
101	Geologic field trips in western Oregon and southwestern Washington. 1980	10.00	
102	Bibliography of geology and mineral resources of Oregon (7th supplement, 1976-79). 1981	5.00	
103	Bibliography of geology and mineral resources of Oregon (8th supplement, 1980-84). 1987	8.00	

MISCELLANEOUS PAPERS

5	Oregon's gold placers. 1954	2.00	
11	Articles on meteorites (reprints from the *Ore Bin*). 1968	4.00	
15	Quicksilver deposits in Oregon. 1971	4.00	
19	Geothermal exploration studies in Oregon, 1976. 1977	4.00	
20	Investigations of nickel in Oregon. 1978	6.00	

SHORT PAPERS

25	Petrography of Rattlesnake Formation at type area. 1976	4.00	
27	Rock material resources of Benton County. 1978	5.00	

OREGON GEOLOGY
Suite 965, 800 NE Oregon Street # 28, Portland, OR 97232

Second Class Matter
POSTMASTER: Form 3579 requested

AVAILABLE DEPARTMENT PUBLICATIONS (continued)

SPECIAL PAPERS — Price √

- 2 Field geology, SW Broken Top quadrangle. 1978 — 5.00 ___
- 3 Rock material resources, Clackamas, Columbia, Multnomah, and Washington Counties. 1978 — 8.00 ___
- 4 Heat flow of Oregon. 1978 — 4.00 ___
- 5 Analysis and forecasts of demand for rock materials. 1979 — 4.00 ___
- 6 Geology of the La Grande area. 1980 — 6.00 ___
- 7 Pluvial Fort Rock Lake, Lake County. 1979 — 5.00 ___
- 8 Geology and geochemistry of the Mount Hood volcano. 1980 — 4.00 ___
- 9 Geology of the Breitenbush Hot Springs quadrangle. 1980 — 5.00 ___
- 10 Tectonic rotation of the Oregon Western Cascades. 1980 — 4.00 ___
- 11 Theses and dissertations on geology of Oregon. Bibliography and index, 1899-1982. 1982 — 7.00 ___
- 12 Geologic linears, N part of Cascade Range, Oregon. 1980 — 4.00 ___
- 13 Faults and lineaments of southern Cascades, Oregon. 1981 — 5.00 ___
- 14 Geology and geothermal resources, Mount Hood area. 1982 — 8.00 ___
- 15 Geology and geothermal resources, central Cascades. 1983 — 13.00 ___
- 16 Index to the *Ore Bin* (1939-1978) and *Oregon Geology* (1979-1982). 1983 — 5.00 ___
- 17 Bibliography of Oregon paleontology, 1792-1983. 1984 — 7.00 ___
- 18 Investigations of talc in Oregon. 1988 — 8.00 ___
- 19 Limestone deposits in Oregon. 1989 — 9.00 ___
- 20 Bentonite in Oregon: Occurrences, analyses, and economic potential. 1989 — 7.00 ___
- 21 Field geology of the NW¼ Broken Top 15-minute quadrangle, Deschutes County. 1987 — 6.00 ___
- 22 Silica in Oregon. 1990 — 8.00 ___
- 23 Forum on the Geology of Industrial Minerals, 25th, 1989, Proceedings. 1990 — 10.00 ___
- 24 Index to the first 25 Forums on the Geology of Industrial Minerals, 1965-1989. 1990 — 7.00 ___

OIL AND GAS INVESTIGATIONS

- 3 Preliminary identifications of Foraminifera, General Petroleum Long Bell #1 well. 1973 — 4.00 ___
- 4 Preliminary identifications of Foraminifera, E.M. Warren Coos County 1-7 well. 1973 — 4.00 ___
- 5 Prospects for natural gas, upper Nehalem River Basin. 1976 — 6.00 ___
- 6 Prospects for oil and gas, Coos Basin. 1980 — 10.00 ___
- 7 Correlation of Cenozoic stratigraphic units of western Oregon and Washington. 1983 — 9.00 ___
- 8 Subsurface stratigraphy of the Ochoco Basin, Oregon. 1984 — 8.00 ___
- 9 Subsurface biostratigraphy of the east Nehalem Basin. 1983 — 7.00 ___
- 10 Mist Gas Field: Exploration/development, 1979-1984. 1985 — 5.00 ___
- 11 Biostratigraphy of exploratory wells, western Coos, Douglas, and Lane Counties. 1984 — 7.00 ___
- 12 Biostratigraphy, exploratory wells, N Willamette Basin. 1984 — 7.00 ___
- 13 Biostratigraphy, exploratory wells, S Willamette Basin. 1985 — 7.00 ___
- 14 Oil and gas investigation of the Astoria Basin, Clatsop and northernmost Tillamook Counties, 1985 — 8.00 ___
- 15 Hydrocarbon exploration and occurrences in Oregon. 1989 — 8.00 ___
- 16 Available well records and samples, onshore/offshore. 1987 — 6.00 ___
- 17 Onshore-offshore cross section, from Mist Gas Field to continental shelf and slope. 1990 — 10.00 ___

MISCELLANEOUS PUBLICATIONS

- Geological highway map, Pacific Northwest region, Oregon, Washington, and part of Idaho (published by AAPG). 1973 — 6.00 ___
- Oregon Landsat mosaic map (published by ERSAL, OSU). 1983 — 11.00 ___
- Geothermal resources of Oregon (published by NOAA). 1982 — 4.00 ___
- Index map of available topographic maps for Oregon published by the U.S. Geological Survey — Free ___
- Bend 30-minute quadrangle geologic map and central Oregon High Cascades reconnaissance geologic map. 1957 — 4.00 ___
- Lebanon 15-minute quad., Reconnaissance geologic map. 1956 — 4.00 ___
- Mist Gas Field Map, showing well locations, revised 1991 (Open-File Report O-91-1, ozalid print, incl. production data) — 8.00 ___
- Northwest Oregon, Correlation Section 24. Bruer and others, 1984 (published by AAPG) — 6.00 ___
- Oregon rocks and minerals, a description. 1988 (DOGAMI Open-File Report O-88-6; rev. ed. of Miscellaneous Paper 1) — 6.00 ___
- Mining claims (State laws governing quartz and placer claims) — Free ___
- Back issues of *Ore Bin/Oregon Geology*, 1939-April 1988 — 1.00 ___
- Back issues of *Oregon Geology*, May/June 1988 and later — 2.00 ___
- Color postcard: Oregon State Rock and State Gemstone — 1.00 ___

Separate price lists for open-file reports, tour guides, recreational gold mining information, and non-Departmental maps and reports will be mailed upon request. The Department also sells Oregon topographic maps published by the U.S. Geological Survey.

ORDER AND RENEWAL FORM

Check desired publications in list above and enter total amount below. Send order to The Nature of Oregon Information Center, Suite 177, 800 NE Oregon Street, Portland, OR 97232, or to FAX (503) 731-4066. Payment must accompany orders of less than $50. Payment in U.S. dollars only. Publications are sent postpaid. All sales are final. Subscription price for *Oregon Geology*: $8 for 1 year, $19 for 3 years.

Amount enclosed: $_____._____ for (check appropriate space):
Publications marked above___. Renewal of current subscription___ / new subscription___ to *Oregon Geology.*

Name _____
Address _____
City/State/Zip _____

Please charge to Visa__ / Mastercard__, account number: ☐☐☐☐ ☐☐☐☐ ☐☐☐☐ ☐☐☐☐

Expiration date: ☐☐ ☐☐

Cardholder's signature _____